POLITECNICO DI TORINO

Collegio di Ingegneria Chimica e dei Materiali

Corso di Laurea Magistrale in Ingegneria Chimica e dei Processi Sostenibili

Tesi di Laurea Magistrale

Process design of a catalytic ammonia cracker for hydrogen generation

Relatore

Prof. Stefania Specchia

Prof. Marcus Rose

Studente

Bruna Nespola

A.A 2025 - 2026

Abstract

The global transition toward a low-carbon economy identifies hydrogen (H_2) as a fundamental energy vector. However, critical challenges related to long-distance storage and transport limit its implementation on a global scale. In this context, ammonia (NH_3) emerges as a strategic hydrogen carrier due to its high volumetric hydrogen density, ease of liquefaction, and well-established global logistics infrastructure. This thesis analyses the process design and simulation in Aspen Plus of a catalytic ammonia cracking process to produce 5 tons/day of high-purity hydrogen (99.9%). Given the strongly endothermic nature of the reaction, the study focuses on comparing two heat supply strategies: conventional thermal heating via combustion and electrical heating. Regarding thermal heating, three combustion scenarios were evaluated (combustion of pure NH_3, pure H_2, or a mixture of both), integrating flammability limit studies with an analysis of nitrogen oxide (NO_x) formation. The combustion of the hydrogen-ammonia mixture proved to be the most promising thermal configuration. Finally, the economic analysis highlights the superiority of electrical heating, with an LCOH of 4,87 €/kg_{H_2} compared to 6,45 €/kg_{H_2} for conventional thermal heating, confirming process electrification as the optimal solution for competitive hydrogen generation.

Acknowledgment

I would like to express my deepest gratitude to the Technische Universität Darmstadt for hosting me during my master thesis and for providing the necessary resources to conduct this research.

A special thanks goes to Professor Marcus Rose and PhD student Tobias Wittmann. Their constant guidance, technical support, and kind availability were key points of reference throughout my research process and the development of this work; without their invaluable contribution, this project would not have been possible.

I would like to extend my special thanks to my supervisor, Professor Stefania Specchia, for her confidence in my work and for facilitating the international collaboration that underpinned this project. Finally, I am grateful to the Politecnico di Torino for making this experience possible, which profoundly enriching from both a personal and professional perspective.

Sommario

List of Figures

List of Tables

Introduzione

Nel contesto globale della decarbonizzazione, l'idrogeno si è affermato come il principale vettore energetico per raggiungere l'obiettivo delle emissioni nette zero entro il 2050. Tuttavia, la sua diffusione a livello mondiale deve affrontare una sfida fondamentale che va oltre la semplice produzione: la logistica. Anche se l'idrogeno è l'elemento più abbondante nell'universo, le difficoltà legate al suo stoccaggio e trasporto rendono necessario l'uso di vettori intermedi più pratici.

In questo scenario, l'ammoniaca (NH_3) gioca un ruolo strategico. A differenza dell'idrogeno puro, l'ammoniaca dispone di un'infrastruttura commerciale già ben sviluppata e di una densità energetica che facilita la sua movimentazione a livello globale. Tuttavia, il limite storico risiede nel suo metodo di produzione: il tradizionale processo Haber-Bosch, che utilizza idrogeno da reforming (SMR), genera circa 420 milioni di tonnellate di CO_2 all'anno.

In questo contesto, l'ammoniaca non è solo un prodotto chimico a basse emissioni, ma diventa un vero e proprio catalizzatore della transizione energetica. Essa funge da vettore di idrogeno, permettendo uno stoccaggio e un trasporto più sicuri ed efficienti rispetto all'idrogeno molecolare. Poiché l'obiettivo finale è l'utilizzo dell'idrogeno da parte dell'utente finale, la catena del valore deve necessariamente includere una fase di riconversione. Una volta arrivata a destinazione, l'ammoniaca viene utilizzata come "serbatoio chimico" da cui estrarre nuovamente i componenti originali — idrogeno e azoto — attraverso il processo di cracking.

In questa prospettiva, il presente lavoro si concentra sull'analisi di un processo integrato per rigenerare l'idrogeno attraverso il cracking dell'ammoniaca, sviluppando una modellazione e una simulazione dettagliata tramite il software Aspen Plus (versione 14.5), adottando un approccio termodinamico e cinetico rigoroso.

In particolare, la decomposizione dell'ammoniaca è stata realizzata in due reattori catalitici, dove la reazione di cracking è stata descritta tramite il modello cinetico di Temkin-Pyzhev, un riferimento consolidato per rappresentare con precisione le reazioni eterogenee su catalizzatori solidi. Per ottimizzare l'intero ciclo, a valle dei reattori, è prevista una sezione dedicata all'assorbimento e alla rigenerazione, per rimuovere l'ammoniaca non convertita dal flusso di reazione. L'ammoniaca viene assorbita in una soluzione costituita principalmente da acqua e acido solforico. La corrente liquida rigenerata viene quindi reintrodotta alla sommità dell'assorbitore in controcorrente rispetto al flusso gassoso, instaurando un ciclo dinamico continuo di assorbimento. Infine, il sistema include una sezione di purificazione dell'idrogeno, progettata per eliminare l'azoto residuo (N_2) e raggiungere il grado di purezza richiesto.

Un aspetto chiave dello studio è l'analisi di due scenari diversi per la fornitura del calore necessario alla reazione di cracking, fortemente endotermica. Il primo scenario prevede il riscaldamento tramite combustione, analizzando tre sotto-casi: la combustione di sola ammoniaca, di solo idrogeno o di una miscela dei due vettori. Per ciascuna di queste configurazioni, sono state stimate le emissioni di ossidi di azoto (NO_x), consentendo una valutazione ambientale comparativa per identificare la soluzione meno inquinante. Il secondo

scenario, invece, considera il riscaldamento elettrico, una soluzione che rappresenta la completa elettrificazione dell'impianto e la possibilità di essere alimentata interamente da fonti energetiche rinnovabili.

Dopo aver completato l'analisi, lo studio si concentra sul calcolo del Levelized Cost of Hydrogen (LCOH), espresso in €/kg_{H_2}. Questo indicatore rappresenta il costo totale necessario per produrre 1 kg di idrogeno durante l'intero ciclo di vita dell'impianto, tenendo conto sia dei costi di investimento che di quelli operativi ed energetici. In questo modo, è possibile confrontare le diverse configurazioni non solo dal punto di vista tecnico, ma anche sotto l'aspetto economico-finanziario.

In sintesi, la tesi è organizzata come segue:

- Una panoramica generale sui componenti (idrogeno, azoto, ammoniaca) e un confronto con i vettori energetici tradizionali.
- L'implementazione del processo su Aspen Plus, con dettagli sui modelli termodinamici, cinetici e specifiche delle apparecchiature.
- Un confronto tra configurazioni (elettrica vs combustione) e un'analisi delle emissioni di NO_x.
- Il calcolo del LCOH finale.

CAPITOLO 1

Principali composti nel cracking dell'ammoniaca e confronto tra vettori energetici

Il primo capitolo di questo lavoro ha l'obiettivo di fornire un'analisi sistematica dei principali composti chimici coinvolti nel processo simulato, con particolare attenzione alle loro proprietà termofisiche e ai rischi legati alla loro manipolazione.

1.1 Ammoniaca

Partendo dall'ammoniaca, questa si distingue per la sua geometria piramidale trigonale e l'alta polarità, che favorisce la formazione di legami a idrogeno, permettendole di liquefarsi a soli 0,8 MPa a temperatura ambiente o a -33 °C a pressione atmosferica. Con un calore latente di vaporizzazione di 1371 kJ/kg, molto superiore a quello della benzina, offre un'eccezionale densità energetica volumetrica, nonostante un LHV di 18,8 MJ/kg.

1.2 Idrogeno

D'altra parte, l'idrogeno molecolare rappresenta l'obiettivo finale della transizione, vantando la più alta densità energetica gravimetrica conosciuta, con un LHV di 120.000 kJ/kg. Tuttavia, la sua bassissima densità presenta enormi sfide: per lo stoccaggio, è necessario

comprimere fino a 700 bar in serbatoi compositi avanzati o mantenere temperature criogeniche di -252,9 °C per la forma liquida. Inoltre, il suo ampio intervallo di esplosività (4-76% in aria) richiede protocolli di sicurezza molto più severi rispetto ai combustibili tradizionali.

1.3 Vettori Energetici: LOCH (liquid organic hydrogen carriers) e metanolo

Oltre all'idrogeno molecolare e all'ammoniaca, lo studio esamina anche altri vettori chimici comuni, come il metanolo e i vettori organici liquidi di idrogeno (LOHC). Il metanolo è vantaggioso per la sua stabilità liquida, ma il suo processo di reforming produce CO_2, mentre i LOHC necessitano di complessi cicli di idrogenazione-deidrogenazione che ne diminuiscono l'efficienza. In sintesi, l'ammoniaca si distingue come la soluzione ideale grazie a una densità volumetrica di 121 kg_{H_2}/m^3 e all'assenza totale di carbonio. La sua forza sta nell'equilibrio tra favorevoli proprietà termodinamiche e la possibilità di utilizzare un'infrastruttura globale già ben sviluppata per il trasporto a lungo raggio.

CAPITOLO 2

Fondamenti della decomposizione dell'ammoniaca: studio su cinetica, catalisi e tecnologie di riscaldamento

Il secondo capitolo offre una panoramica teorica sui meccanismi che governano la decomposizione dell'ammoniaca, partendo dalle basi termodinamiche fino alla scelta dei sistemi catalitici e delle configurazioni dei reattori.

La decomposizione dell'ammoniaca è una reazione endotermica, descritta dall'equilibrio:

$$2NH_3 \leftrightarrow N_2 + 3H_2$$

con un'entalpia standard di reazione pari a $\Delta H^\circ = 91.2$ kJ/mol. Per ottenere elevate conversioni, è fondamentale operare a temperature tra i 500 °C e i 700 °C, sfruttando il fatto che la reazione è favorita da basse pressioni e alte temperature, secondo il principio di Le Chatelier. La trasformazione avviene sulla superficie del catalizzatore attraverso stadi sequenziali: l'adsorbimento dell'ammoniaca, la scissione dei legami N-H e il successivo desorbimento dell'azoto e dell'idrogeno molecolare.

Per descrivere questo comportamento nelle simulazioni di Aspen Plus, la letteratura indica il modello di Temkin-Pyzhev come il più rigoroso, capace di rappresentare la velocità di reazione tenendo conto della natura eterogenea del catalizzatore. In questo studio, la cinetica è stata implementata seguendo l'equazione di Arrhenius, con un'energia di attivazione apparente di 120.000 kJ/kmol.

2.1 Catalizzatori per la decomposizione catalitica dell'ammoniaca

Per quanto riguarda i catalizzatori, partendo dai metalli nobili, il Rutenio (Ru) si distingue come un punto di riferimento per le sue prestazioni, grazie alla sua abilità di bilanciare perfettamente l'adsorbimento e il desorbimento dell'azoto. Tuttavia, il suo costo elevato ha spinto la ricerca verso metalli di transizione più accessibili. Anche se il Ferro (Fe) è stato storicamente utilizzato per rimuovere l'ammoniaca dai gas di scarico, la sua tendenza a formare nitruri superficiali stabili rende complicato il suo utilizzo per la produzione di idrogeno puro. Il Cobalto (Co) emerge come un'alternativa promettente per le sue proprietà di adsorbimento, ma necessita ancora di ottimizzazioni per un uso industriale su larga scala.

Un ulteriore sistema catalitico di interesse è rappresentato dal Nickel (Ni). La letteratura sottolinea come la sua attività sia estremamente sensibile alla morfologia e alla dimensione delle particelle (ottimali sotto i 2,9 nm) e come la scelta del supporto sia cruciale per evitare il "sintering" durante le operazioni ad alta temperatura. Sulla base del miglior compromesso tra efficienza catalitica, disponibilità commerciale e stabilità nel tempo, il Nickel è stato scelto come benchmark per la modellazione dei reattori in ambiente Aspen Plus.

2.2 Configurazioni reattoristiche e strategie di riscaldamento per il cracking dell'ammoniaca

Una volta definito il sistema catalitico, l'attenzione si sposta sulla progettazione del reattore, che deve garantire un trasferimento di calore efficiente per sostenere la reazione endotermica. In letteratura, si esplorano diverse configurazioni, dai reattori a letto fisso a quelli a membrana, fino ai sistemi integrati con riscaldamento elettrico o a combustione. Questo lavoro di tesi analizza due scenari:

- Riscaldamento tramite Combustione: È la strategia tradizionale che prevede l'uso di un bruciatore. Il calore viene prodotto dalla combustione di una parte dei gas di processo. Qui, questo approccio viene approfondito in tre sotto-casi: la combustione di sola ammoniaca, di solo idrogeno o di una miscela di entrambi. La principale sfida di questa configurazione è la gestione delle emissioni di ossidi di azoto (NO_x), che vengono simulate (con Aspen Plus) per valutarne l'impatto ambientale.
- Riscaldamento Elettrico: In questa configurazione, il calore è fornito tramite resistenze elettriche o sistemi a induzione, eliminando le emissioni dirette e consentendo l'integrazione diretta con fonti rinnovabili.

CAPITOLO 3

Modellazione e simulazione del processo di cracking dell'ammoniaca in Aspen Plus

Il terzo capitolo descrive la fase operativa del lavoro, ovvero la modellazione e simulazione del processo di cracking dell'ammoniaca realizzata nel software Aspen Plus.

L'obiettivo principale dell'impianto è convertire l'ammoniaca liquida in un flusso di idrogeno ad alta purezza (> 99,9 %) attraverso un ciclo integrato e termicamente efficiente, in grado di minimizzare il consumo di energia esterna. Il flowsheet è stato progettato per una capacità produttiva di riferimento di 5 tonnellate di idrogeno al giorno, a fronte di un'alimentazione di 38 tonnellate di ammoniaca al giorno.

3.1 Selezione dei modelli termodinamici in Aspen Plus

Per garantire una simulazione accurata, è fondamentale selezionare modelli termodinamici rigorosi per calcolare le proprietà chimico-fisiche e i cambiamenti entalpici del sistema. In Aspen Plus, è stato adottato un approccio ibrido basato su due modelli principali:

- ELECNRTL (Electrolyte Non-Random Two-Liquid): Questo modello è cruciale per descrivere la sezione di assorbimento, dove l'ammoniaca residua viene eliminata attraverso un processo di assorbimento chimico in una soluzione di acido solforico (H_2SO_4). ELECNRTL gestisce con grande precisione i sistemi liquidi non ideali che contengono specie ioniche, calcolando le forze a lungo e corto raggio tra gli ioni e le molecole neutre. Per modellare in modo accurato la solubilità dei gas volatili come NH_3, N_2, H_2, queste specie sono state scelte come Componenti di Henry.
- Peng-Robinson (PR): Per le sezioni ad alta temperatura, come i reattori di cracking e le parti dell'impianto dominate dalla fase gassosa, è stata utilizzata l'equazione di stato di Peng-Robinson. Essendo un'equazione cubica, PR assicura un'elevata accuratezza nel calcolo di densità, entalpia e fugacità per la miscela gassosa di idrogeno e azoto in condizioni di reazione, oltre a prevedere correttamente l'equilibrio vapore-liquido (VLE).

3.2 Simulazione del processo di cracking dell'ammoniaca: analisi del flowsheet

Il cuore del processo è rappresentato dalla sezione di reazione configurata con due reattori catalitici disposti in serie, intervallati da uno stadio di riscaldamento intermedio [Figura 16]. L'ammoniaca viene inizialmente preriscaldata nello scambiatore HE1, sfruttando il calore recuperato dalle correnti di processo già presenti nel ciclo. Questa strategia di integrazione

termica è fondamentale per ridurre il fabbisogno di utenze esterne e aumentare l'efficienza complessiva del ciclo. La configurazione con due reattori in serie e riscaldamento intermedio è stata scelta per minimizzare la potenza termica complessiva richiesta dal processo di cracking. Come mostrano i risultati della simulazione [Figura 17], questa soluzione consente una significativa riduzione del calore totale da fornire al sistema: la potenza richiesta si attesta infatti intorno a 1450 kW, rispetto agli oltre 1850 kW necessari nel caso di una configurazione a reattore singolo.

L'effluente che esce dal secondo reattore è una miscela di idrogeno, azoto e una piccola quantità di ammoniaca non convertita. Per raggiungere una purezza superiore al 99,9%, il gas viene compresso a 19 atm e raffreddato a 100 °C prima di passare alla sezione di purificazione. Qui, un sistema integrato di assorbimento e stripping si occupa di eliminare le tracce di ammoniaca. La soluzione assorbente, composta da acqua e acido solforico, viene poi rigenerata e ricircolata nella colonna di assorbimento, permettendo un ciclo continuo di rimozione dell'ammoniaca e ottimizzando l'efficienza del processo.

Il flusso che esce dall'assorbitore, ora quasi completamente formato da idrogeno e azoto, viene inviato all'unità PSA (Pressure Swing Adsorption). Questo sistema di purificazione avanzata consente la rimozione selettiva dell'azoto (N_2), assicurando un flusso di idrogeno con il grado di purezza finale richiesto dalle specifiche industriali e una capacità produttiva di 5 tonnellate al giorno.

CAPITOLO 4

H_2 e NH_3 come combustibili verdi per il processo di cracking dell'ammoniaca

Il Capitolo 4 è dedicato all'analisi comparativa delle principali strategie di riscaldamento del reattore necessarie per sostenere la natura fortemente endotermica della reazione di cracking dell'ammoniaca. Mentre il riscaldamento elettrico rappresenta l'avanguardia tecnologica per l'integrazione con le fonti rinnovabili, la combustione rimane una soluzione fondamentale per l'industria, a condizione di utilizzare vettori energetici a zero emissioni di carbonio.

4.1 Strategie di riscaldamento del reattore mediante combustione di idrogeno, ammoniaca e miscele H_2-NH_3

Per quanto riguarda la strategia basata sulla combustione, l'analisi si è concentrata sull'uso di combustibili che non emettono anidride carbonica, rendendo il processo intrinsecamente "green". In questa prospettiva, per evitare l'introduzione di combustibili esterni e mantenere il sistema il più autosufficiente possibile, è stata considerata la combustione di composti già presenti nel processo, come idrogeno e ammoniaca. Una delle soluzioni esplorate prevede l'uso

di una parte dell'idrogeno prodotto internamente per alimentare il bruciatore. Questa opzione è particolarmente affascinante grazie alle straordinarie proprietà chimico-fisiche dell'idrogeno, che offre un'alta densità energetica e una velocità di fiamma superiore rispetto ai combustibili fossili tradizionali. Questo garantisce una combustione stabile, producendo solo vapore acqueo come sottoprodotto.

In alternativa, lo studio considera l'uso dell'ammoniaca stessa come combustibile, focalizzandosi sul flusso della sezione di purificazione, chiamato PROD-AMM. Tuttavia, a causa della bassa velocità di fiamma e dell'alta temperatura di autoaccensione dell'ammoniaca, è stata esaminata anche una terza configurazione ibrida: la combustione di miscele di idrogeno e ammoniaca. Questa soluzione cerca di unire i vantaggi di entrambi i vettori, utilizzando l'idrogeno come "catalizzatore" per migliorare la reattività dell'ammoniaca, assicurando così una fiamma più stabile e una gestione termica più flessibile del reattore.

4.2 Valutazione della combustione di H_2, NH_3 e miscele H_2-NH_3 tramite reattore RGibbs in Aspen Plus

Al fine di individuare la miscela con il minore impatto ambientale, il processo di combustione è stato simulato in Aspen Plus mediante un reattore di tipo RGibbs. Tale approccio consente di determinare la composizione dei prodotti all'equilibrio termodinamico attraverso la minimizzazione dell'energia libera di Gibbs del sistema, senza richiedere la definizione di un meccanismo cinetico dettagliato. Questo è cruciale per prevedere con precisione la formazione degli ossidi di azoto (NO_x), che si generano inevitabilmente a causa delle alte temperature e della presenza di azoto e aria. Infatti, poiché queste reazioni avvengono in tali condizioni, il monitoraggio di questi inquinanti diventa un parametro chiave per valutare la sostenibilità complessiva del sistema.

Dopo aver effettuato diverse simulazioni, è emerso che la miscela di idrogeno e ammoniaca è quella con il maggior potenziale. Questa configurazione consente di bilanciare le temperature della fiamma, mantenendo la formazione di NO_x entro limiti ottimali [Tabella 11], il che si traduce in un minore impatto ambientale. I risultati sono promettenti; mostrano valori di ossidi di azoto estremamente bassi: NO ≈ 0,0004 ppm e $NO_2 \approx 3{,}46 \cdot 10^{-12}$ ppm, il che conferma l'efficacia di questa strategia.

CAPITOLO 5

Analisi economica e valutazione del costo livellato dell'idrogeno (LCOH)

Nel Capitolo 5, la tesi si conclude con un'analisi economica che mira a valutare la sostenibilità finanziaria delle soluzioni tecnologiche simulate, utilizzando il calcolo del Levelized Cost of Hydrogen (LCOH). Questo parametro è cruciale perché traduce i dati tecnici e termodinamici in una metrica di costo che è possibile confrontare, rivelando quanto costa realmente produrre un chilogrammo di idrogeno in base alla configurazione scelta.

5.1 Analisi economica: CAPEX e OPEX per riscaldamento a combustione ed elettrico

L'analisi economica confronta due configurazioni: il riscaldamento tramite combustione tradizionale e quello elettrico. I costi sono stati suddivisi in CAPEX (Capital Expenditure), che riguardano gli investimenti iniziali per le attrezzature, e OPEX (Operating Expenditure), che si riferiscono ai costi di gestione annuali.

Un aspetto interessante è la differenza nei flussi di materia prima necessari per garantire lo stesso output netto di 5 tonnellate al giorno di idrogeno. Nella configurazione a combustione, si nota un aumento dell'OPEX a causa della necessità di alimentare il bruciatore: per compensare la frazione di flusso deviata verso la combustione, l'input di ammoniaca deve aumentare a tonnellate/giorno, rispetto alle 38 tonnellate/giorno del caso elettrico. Questo surplus di materia prima non solo aumenta i costi variabili, ma ha anche un impatto sul CAPEX, poiché gestire portate di massa più elevate richiede un dimensionamento maggiore di tutte le attrezzature dell'impianto. Inoltre, nel caso della combustione, è necessario considerare il costo specifico per l'installazione della fornace, che è una spesa esclusiva di questa configurazione.

Per quanto riguarda la configurazione elettrica, l'analisi del CAPEX si concentra sui costi del sistema di riscaldamento integrato nel reattore. In questo scenario, anche se i costi della materia prima (ammoniaca) sono inferiori grazie al minor input richiesto (38 t/d), l'OPEX è influenzato dal costo dell'energia elettrica necessaria per sostenere la reazione endotermica.

5.2 Valutazione del Levelized Cost of Hydrogen (LCOH) per riscaldamento elettrico e a combustione

Il calcolo finale del Levelized Cost of Hydrogen (LCOH), espresso in €/kg_{H_2}, consente di identificare la soluzione più economica traducendo l'efficienza tecnica in termini finanziari. Dall'analisi effettuata, emergono valori distinti per i due scenari: la configurazione basata sul riscaldamento elettrico ha restituito un valore di LCOH pari a 4,87 45 €/kg_{H_2}, mentre quella che utilizza il riscaldamento tramite combustione ha presentato un costo leggermente superiore, attestandosi su 6,45 €/kg_{H_2}.

Sebbene questo studio rappresenti un'analisi preliminare e non un bilancio completo del ciclo di vita (LCA), fornisce indicazioni importanti per futuri studi di fattibilità tecnico-

economica. In sintesi, il capitolo dimostra che la scelta strategica migliore per il riscaldamento del reattore di cracking è quella elettrica. Questa configurazione risulta la più vantaggiosa non solo per l'assenza di emissioni dirette, ma soprattutto perché garantisce il minor valore di LCOH, confermando che l'elettrificazione del processo rappresenta la via più efficiente e competitiva per la produzione di idrogeno da ammoniaca verde.

5.3 Competitività economica dell'idrogeno verde rispetto a quello fossile

Secondo il *Global Hydrogen Review* 2025, nel 2022, a causa della guerra in Ucraina, i prezzi del gas hanno subito un'impennata, portando il costo dell'idrogeno da fonti fossili a circa 9 $/kg$_{H_2}$. Questo ha reso l'idrogeno verde competitivo per la prima volta. Tuttavia, all'epoca non c'erano impianti di produzione di idrogeno verde in grado di sostituire il gas naturale.

Nei due anni successivi, i prezzi del gas sono scesi, riportando il costo dell'idrogeno fossile a un intervallo tra 0,8 e 4 $/kg$_{H_2}$, mentre l'industria dell'idrogeno verde ha affrontato sfide legate all'aumento dei costi delle materie prime e alla lentezza nell'implementazione di nuove tecnologie.

In questo contesto, l'analisi indica che l'idrogeno prodotto tramite combustione ha un costo leggermente superiore a 6 €/kg$_{H_2}$ (circa 5 $/kg$_{H_2}$), mentre nel caso del riscaldamento elettrico il LCOH scende a poco più di 4 €/kg$_{H_2}$ (circa 4,2 $/kg$_{H_2}$). Considerando il range di prezzo dell'idrogeno fossile (0,8–4 $/kg$_{H_2}$), il valore ottenuto per la configurazione elettrica suggerisce che, almeno in teoria, la produzione di idrogeno verde potrebbe già risultare competitiva rispetto alle tecnologie tradizionali.

Conclusioni e prospettive future

Lo studio si è focalizzato sull'analisi comparativa di due strategie diverse per l'alimentazione termica del reattore di cracking. Da un lato, abbiamo il processo tradizionale a combustione, noto per generare inquinanti come gli ossidi di azoto (NO_x), e dall'altro, il riscaldamento elettrico. È emerso che, se si sceglie la combustione, la soluzione più promettente per ridurre le emissioni di gas serra e altre sostanze inquinanti è l'uso di una miscela di idrogeno e ammoniaca.

I risultati sul calcolo del LCOH (Levelized Cost of Hydrogen) mostrano che la configurazione con riscaldamento elettrico non solo elimina le emissioni in atmosfera, ma ha anche costi di produzione inferiori rispetto al metodo tradizionale. In conclusione, il cracking dell'ammoniaca alimentato elettricamente si rivela una scelta migliore sia per l'ambiente che per l'economia, con valori di LCOH molto competitivi rispetto alla produzione convenzionale da fonti fossili. Questo aspetto offre spunti significativi per progettare nuovi impianti industriali

che puntano a eliminare completamente l'uso di combustibili fossili nella filiera dell'idrogeno, contribuendo così a raggiungere gli obiettivi climatici fissati per il 2050.

I risultati ottenuti aprono anche a diverse considerazioni necessarie per un futuro passaggio alla scala industriale. In primo luogo, l'evoluzione del lavoro dovrà concentrarsi sull'ottimizzazione del sistema di purificazione per adsorbimento: nel modello attuale, la Pressure Swing Adsorption (PSA) è stata considerata come un separatore ideale, mentre una nuova analisi dovrebbe includere lo sviluppo di cicli di adsorbimento specifici o l'uso di membrane selettive. Questo aspetto è davvero cruciale, perché l'idrogeno destinato alle celle a combustibile richiede una purezza molto elevata, e l'energia necessaria per le fasi di separazione potrebbe avere un impatto significativo sul calcolo finale del LCOH.

Allo stesso tempo, la validazione del processo richiederà un'analisi approfondita della dinamica e della variabilità delle fonti rinnovabili. Dato che il riscaldamento elettrico del reattore si basa su energia solare ed eolica, sarà fondamentale valutare come il sistema risponde alle fluttuazioni del carico energetico e se sarà necessario implementare sistemi di accumulo termico per garantire un'operatività stabile e continua.

Dal punto di vista economico, considerando che l'LCOH del caso elettrico è estremamente sensibile al prezzo del kWh, future ricerche potrebbero esaminare la convenienza del processo in diverse aree geografiche. Sarebbe particolarmente interessante analizzare la competitività della tecnologia in mercati con costi energetici differenti, come l'Italia, ma anche in regioni come il Nord Africa o il Cile, dove l'abbondanza di risorse solari potrebbe ridurre drasticamente i costi di produzione.

Infine, il passaggio dalla simulazione in Aspen Plus alla costruzione di un impianto pilota richiederà uno studio di scale-up per affrontare le sfide costruttive legate alla resistenza dei materiali alle alte temperature e alla gestione di portate su larga scala, passaggi fondamentali per rendere il cracking dell'ammoniaca una realtà industriale consolidata.

Introduction

In today's global landscape, hydrogen has emerged as a key player in a sustainable, decarbonised future. In fact, it plays a fundamental role in achieving the goal of net-zero emissions by 2050 [1]. The transition from high-carbon fuels to sustainable alternatives is essential to mitigate the negative environmental impacts associated with fossil fuels, such as coal and oil [2].

Hydrogen is considered a potential substitute thanks to its unique characteristics; it is the most abundant element in the universe, it is a carbon free energy carrier and when burned, releases only water as a by-product. Due to its abundance, hydrogen can be produced from a wide range of compounds using various methods, some of which are classified as “green”[3].

However, one of the main challenges of the hydrogen economy is not limited to the production phase, but extends to storage, transport and distribution to the end user, particularly in a global context [4]. This is where ammonia begins to play a key role. It is, in fact, a substance that is already widely traded internationally, supported by a mature and well-established global infrastructure dedicated to its storage, transport and handling.

In terms of transport, the ammonia logistics landscape includes a global port network consisting of 126 specialised terminals, divided into 88 export hubs and 38 import destinations. Among these, six strategic infrastructures are capable of handling both operational flows.

Alternatively, ammonia distribution can be managed via pipeline or maritime transport. For example, a 3,060 km pipeline network connects Texas to Iowa in the United States, while another important 2,420 km infrastructure connects Russia to Ukraine, ensuring the supply of essential raw materials for the fertiliser industry and various chemical complexes [5].

Mainly for transport purposes, but not exclusively, ammonia is emerging as the most promising hydrogen energy carrier of all.

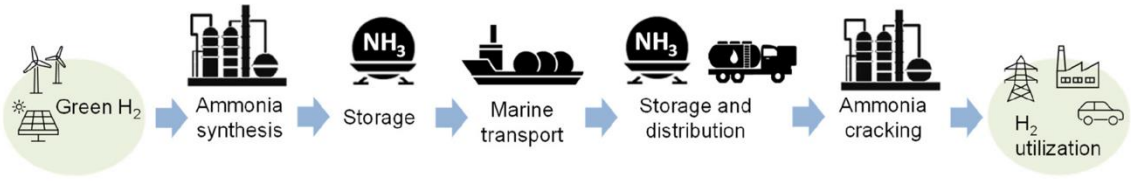

Figure 1: NH_3 value chain as a hydrogen carrier [4].

Figure 1 illustrates the value chain of ammonia as a hydrogen carrier for maritime transport. NH_3 is mainly produced in large-scale industrial plants using the well-known Haber-Bosch process. This process enables the synthesis of ammonia from nitrogen and hydrogen; the latter is generally obtained through steam methane reforming (SMR), which operates at high temperatures and pressures. Since hydrogen is currently derived mainly from fossil sources, conventional NH_3 production contributes significantly to global greenhouse gas emissions (420 million tonnes of CO_2 are emitted each year [4], 2% of global energy demand [5]) .

Consequently, in this specific context—as well as throughout the development of this thesis—reference is made exclusively to ammonia produced from green hydrogen. In particular, hydrogen is obtained through the process of water electrolysis, powered by electricity from renewable sources.

Although water electrolysis is the main focus of this work, green hydrogen can also be synthesized through several other carbon-neutral pathways. These include biological methods, such as biophotolysis and fermentation [6], as well as thermochemical processes such as biomass gasification. The distinctive feature of these approaches is their ability to produce hydrogen with net zero CO_2 emissions.

After being synthesised, ammonia is stored and then transported to its point of use by various means, such as ships (as shown in Figure 1), pipelines, or road and rail transport, to its destination terminal. Upon arrival, the ammonia is converted back into hydrogen and nitrogen through the cracking process. The hydrogen produced is then used in the relevant sectors; in this study, it is mainly considered for chemical applications that require levels of purity exceeding 99.9%.

This work analyses an integrated process for hydrogen production via ammonia cracking, with a particular focus on solutions compatible with energy transition scenarios and the use of green ammonia as an energy carrier. The entire process was modelled and simulated using Aspen Plus software (version 14.5), adopting a rigorous thermodynamic and kinetic approach.

Ammonia decomposition was implemented in two catalytic reactors, in which the cracking reaction was described using a Temkin-Pyzhev kinetic model, commonly used to accurately represent heterogeneous reactions on solid catalysts.

Downstream of the reactor, an absorption and regeneration section has been implemented to remove unconverted ammonia from the reaction stream. The absorbed ammonia is then regenerated and recycled as feedstock to the cracking reactor, thus reducing reagent losses, improving overall process efficiency and minimising raw material waste. The process is then completed with a hydrogen purification section, designed to remove residual nitrogen (N_2) to obtain a high-purity product.

Two different scenarios were analysed for supplying the heat required for the endothermic ammonia cracking reaction. In the first case, the reactor is heated by combustion, while the

second scenario considers electric heating, representative of fully electrified solutions potentially powered by renewable sources.

In the case based on combustion, three different sub-cases were further examined: ammonia combustion, hydrogen combustion and hydrogen-ammonia mixture combustion. For each configuration, nitrogen oxide (NO_x) emissions were estimated using simulations in Aspen Plus, allowing for a comparative environmental assessment and the identification of the most advantageous solution in terms of pollutant reduction.

During the study, numerous sensitivity analyses were conducted on the main operating and design parameters of the equipment involved in the process, with particular attention to the absorption and regeneration columns. These analyses made it possible, for example, to determine the optimal number of equilibrium stages.

Finally, to quantitatively compare the two reactor heating strategies, a simplified preliminary economic analysis was carried out to calculate the Levelized Cost of Hydrogen (LCOH), expressed in €/kg of hydrogen produced. Although this analysis does not include a complete economic assessment of the plant's life cycle, the LCOH parameter allowed for an effective comparison between the two configurations and the identification of the most cost-effective solution from a strictly economic point of view, providing useful information for future more in-depth technical-economic feasibility studies.

Based on the considerations presented so far, the thesis is structured as follows:

First, a general overview of the main components of the process — hydrogen, nitrogen and ammonia — is provided. This is followed by a comparative analysis of traditional energy carriers, highlighting the technical advantages that identify ammonia as the most effective solution.

The study continues with the implementation of the process developed using Aspen Plus software. This section illustrates the thermodynamic and kinetic models adopted, together with the technical specifications of the equipment involved.

Subsequently, the two reactor configurations — electric and combustion-based — are compared, including an assessment of nitrogen oxide (NO_x) emissions. Finally, the Levelized Cost of Hydrogen (LCOH) was calculated for both scenarios in order to identify the most cost-effective solution.

Chapter 1

Key compounds and energy carrier comparison

This chapter provides an overview of the main chemical compounds discussed in this thesis, with a particular focus on hydrogen (H_2) and ammonia (NH_3). The analysis then examines the various energy carriers that are essential for the implementation of a hydrogen-based economy.

1.1 Ammonia

Ammonia (NH_3) is a molecule characterised by a trigonal pyramidal geometry, exhibiting high polarity and the ability to form intermolecular hydrogen bonds [7]. From a thermophysical perspective, it has a boiling point of 239.8 K [8]. A key feature for the use of ammonia as an energy carrier is its relatively high boiling point, which allows liquefaction at moderate pressures (approximately 0.8 MPa at room temperature), similar to propane. In this condition, ammonia can be handled in liquid form in thermally insulated tanks, also exploiting its high latent heat of vaporization (1371 kJ/kg), which is significantly higher than that of gasoline.

Although its lower heating value (LHV) of 18.8 MJ/kg is considerably lower than the 120 MJ/kg of hydrogen, ammonia offers a volumetric energy density and ease of storage that make it highly competitive. Furthermore, with an octane number of approximately 130 and an auto-ignition temperature of 930 K, it exhibits relatively low reactivity. This makes its combustion technically challenging but inherently safer compared to other liquid or gaseous fuels.

1.1.1 Health and Safety (H&S) Considerations

The use of ammonia requires a rigorous assessment of health and safety risks. The National Fire Protection Association (NFPA) classifies ammonia as both a toxic and corrosive substance [9]. Human exposure is strictly regulated: long-term exposure limits (TWA) are generally set between 20 and 50 ppm, while concentrations exceeding 300 ppm are considered immediately dangerous to life or health [8,9].

As shown in Figure 2, the risk profile of ammonia presents unique characteristics compared to traditional fuels. The graph correlates flammability with toxicity (health), highlighting how ammonia occupies an opposite position relative to hydrocarbons such as gasoline, LPG, or methane. While the latter pose a high risk of fire and explosion, ammonia exhibits low ignitibility, shifting the core risk toward human health concerns.

This profile is confirmed by the American NFPA 704 classification shown in the figure, which assigns ammonia a value of 3 for health (high hazard), but only 1 for flammability and 0 for reactivity. This indicates that although the substance requires stringent precautions to prevent inhalation or contact, it is inherently more stable and less prone to catastrophic explosions than fossil fuels or hydrogen.

Despite its toxicity, ammonia possesses a "self-warning" characteristic: its pungent odor is detectable at very low, safe concentrations. Furthermore, being lighter than air, it tends to disperse rapidly upward in the event of gaseous leaks. However, if released as a "flashing" liquid, it can create dense aerosol clouds that remain near ground level, increasing the risk of exposure.

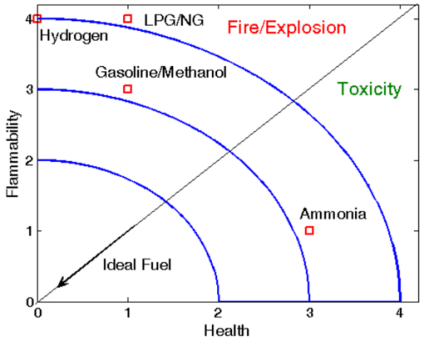

NFPA 704 Classification:

Health	Flammability	Reactivity
3	1	0

Figure 2: Ammonia positioning in the flammability-toxicity diagram and NFPA 704 hazard classification [8].

1.1.2 Flammability and Explosion Risk

Regarding fire risk, anhydrous ammonia is considered non-flammable, yet its vapours can become explosive when mixed with air within a mole fraction range of 18% to 28% [8]. A critical phenomenon to monitor, particularly in large-scale industrial facilities, is the Boiling Liquid Expanding Vapour Explosion (BLEVE), which may occur if storage tanks suffer structural failure due to external heat sources.

Nevertheless, the risk of accidental explosion is mitigated by the high ignition energy required and a low laminar burning rate (less than 0.010 m/s) [6]. These parameters make ammonia significantly less prone to spontaneous explosions compared to common hydrocarbons or hydrogen.

1.1.3 Corrosivity and Material Compatibility

The integration of ammonia into energy systems requires careful selection of materials due to its corrosive effects on copper, brass and zinc alloys. As an alkaline reducing agent, NH_3 is incompatible with halogens and oxidants, necessitating strict adherence to chemical compatibility standards for piping and structural components. Therefore, careful material selection is a crucial design constraint to ensure the structural integrity and safety of ammonia-based energy systems. Corrosive behaviour can be managed with materials such as Hastelloy; however, these are much more expensive than steel [11].

1.2 Hydrogen

Molecular hydrogen (H_2) is a colourless and odourless diatomic gas under standard conditions. Thanks to its extreme versatility, it occupies a prominent position in the global energy landscape: it can be produced both from fossil fuels (through steam methane reforming) and from renewable sources, such as wind and solar energy, through water electrolysis. This dual nature allows hydrogen to act as a fundamental bridge towards decarbonisation, adapting to specific industrial needs [12].

A critical parameter for energy logistics is its high expansion ratio: during the transition from a liquid to a gaseous state, the volume increases approximately 700-fold. Although liquefaction allows for a density of 70.8 g/L ($0.07 g/cm^3$), hydrogen maintains an exceptionally low mass density compared to conventional liquid fuels.

From an energy perspective, hydrogen boasts the highest gravimetric energy density among all known carriers, with a Lower Heating Value (LHV) of 120,000 kJ/kg (32.9 kWh/kg) and a Higher Heating Value (HHV) of 141,900 kJ/kg. However, large-scale application requires rigorous safety protocols due to an extremely wide explosive range (4-76% by volume in air) and an auto-ignition temperature between 773 K and 844 K [12].

1.2.1 Health and Safety (H&S) Considerations

Despite its non-toxic classification, hydrogen presents several physiological safety concerns [15]. In confined areas, leaking gas acts as a simple asphyxiant by driving out atmospheric oxygen. Moreover, handling liquid hydrogen (LH2) at -253°C requires caution due to its cryogenic properties; accidental exposure results in severe frostbite, while the embrittlement of surrounding materials often leads to unexpected structural collapses.

1.2.2 Flammability and Explosion Risk

Hydrogen is classified with the highest flammability rating (NFPA 704: Level 4) due to several critical factors:

i. Wide Flammability Range**:** Hydrogen can combust at concentrations ranging from 4% to 75% by volume in air. The maximum hazard is reached at the stoichiometric mixture (approximately 30%), which is particularly unstable and reactive in enclosed spaces.

ii. Low Minimum Ignition Energy (MIE): A defining risk factor is its extremely low ignition energy (approximately 0.017 mJ). This allows combustion to be triggered by minimal sources, such as static discharge or imperceptible electrical sparks, which would be insufficient to ignite conventional fuels.

iii. Deflagration to Detonation Transition (DDT): In confined environments, hydrogen combustion typically begins as a deflagration (subsonic flame propagation with pressure increase). However, due to its high flame speed, it can rapidly evolve into a detonation—the most destructive form of combustion—where the shock wave exceeds the speed of sound, leading to severe structural overpressure [13].

1.2.3 Corrosivity and Material Compatibility

The technical guide on hydrogen compatibility examines how gaseous hydrogen interacts with structural materials, highlighting two main issues. The first is permeation, which is the ability of hydrogen to move through solid materials, potentially leading to leaks across the structure. The second, and more serious, is the decline in mechanical properties, technically known as Hydrogen-Assisted Fracture (or hydrogen embrittlement). This process directly weakens the structure by making the material less flexible and less tough, which can lead to sudden and dangerous failures when the system is under pressure [17].

1.3 Energy carrier comparison

The transition toward a hydrogen-based economy is strictly tied to the development of storage and transport strategies that are not only safe but also technically and economically viable on a large scale. The main technological challenges in this field stem from the intrinsic properties of the hydrogen molecule, specifically its extremely low volumetric energy density under standard conditions and its high propensity for diffusion, which can lead to the embrittlement of metallic materials used in infrastructure [14].

To overcome these limitations, the solutions currently at the centre of the scientific debate are divided into two fundamental approaches: physical storage and chemical storage via dedicated carriers. Physical solutions, which include hydrogen compressed at high pressures or liquefied at cryogenic temperatures, allow for the direct use of the H_2 molecule without the need for chemical transformations. However, these technologies are limited by high energy costs associated with compression and cooling processes, as well as infrastructural and safety concerns that largely restrict their application to local or short-distance contexts.

On the contrary, the chemical storage of hydrogen involves its incorporation into stable compounds or solid and liquid materials, from which the molecule can be subsequently released through controlled decomposition or dehydrogenation reactions. In this context, chemical carriers (or Hydrogen Carriers) such as ammonia, methanol, and Liquid Organic Hydrogen Carriers (LOHC) emerge as particularly promising solutions. These carriers offer significantly higher volumetric energy density and the possibility of storage under ambient conditions, while ensuring valuable compatibility with existing transport and distribution infrastructures used for fossil fuels. Despite the efficiency losses linked to chemical reconversion processes, these carriers represent a key element today for enabling long-distance transport and large-scale storage of renewable energy on a global level.

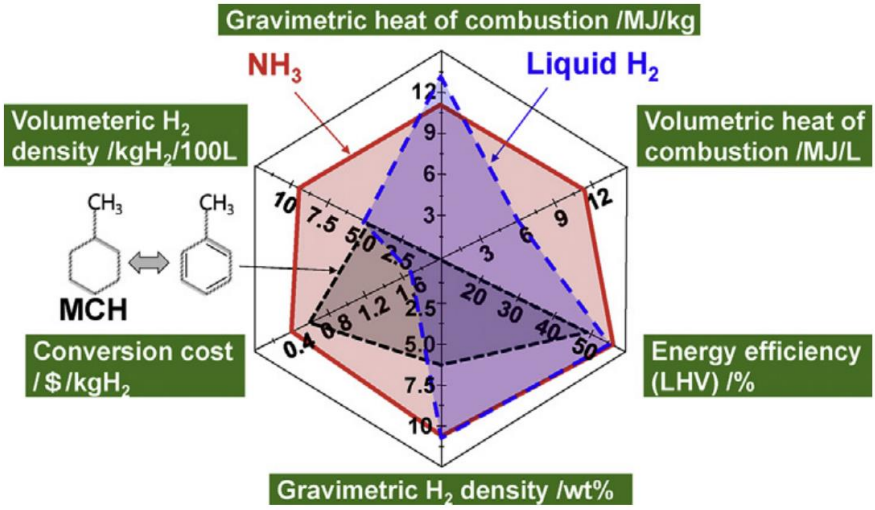

Figure 3: Comparative analysis of hydrogen carriers: NH_3, liquid H_2, and MCH [15].

1.3.1 Compressed hydrogen storage

The most straightforward and technologically mature method for storing hydrogen gas consists of compressing it within pressure vessels. To optimize energy density, hydrogen is typically compressed to values ranging between 350 and 700 bar using tanks made of advanced composite materials [18].

From a thermodynamic point of view, the need to operate at such high pressures is dictated by the nature of the gas itself. According to the ideal gas law at constant temperature and volume, an increase in pressure allows a greater number of moles of hydrogen to be stored in the same space. However, it is important to note that this ideal model is not fully applicable in real operating conditions. At the extremely high pressures required for storage, deviations from ideal behaviour become significant. Consequently, more complex equations of state are needed to accurately describe the behaviour of the fluid.

In addition to thermodynamic challenges, compressed storage presents significant obstacles related to materials science. The extreme mechanical stresses involved necessitate the use of highly resistant containers; currently, four main types of pressure vessels (Types I, II, III, and IV) have been developed [16]:

- Type I: these tanks consist of steel cylinders capable of storing 25 Nm^3 of hydrogen at 12 MPa with a weight of 500 kg.
- Type II: These are designed for pressures less than or equal to 100 MPa and are typically used for stationary high-pressure storage.
- Type III and IV: These types are preferred for use in tube trailers and for integration into containers for hydrogen transport.

The selection of a specific vessel type depends on the field of application, requiring a strategic compromise between technical performance, weight, and manufacturing costs.

1.3.2 Hydrogen Liquefaction

Hydrogen liquefaction allows for higher energy densities but at the cost of an extremely energy-intensive industrial process with modest efficiencies. Since the liquefaction temperature of hydrogen is -252.9 °C, the necessity of operating at such cryogenic temperatures requires a series of complex thermodynamic steps (such as those observed in Figure 4) that heavily weigh on the overall energy balance [17]. This process can consume up to 45% of the energy stored as hydrogen, while additional losses due to boil-off further contribute to the high energy overhead of the system [18].

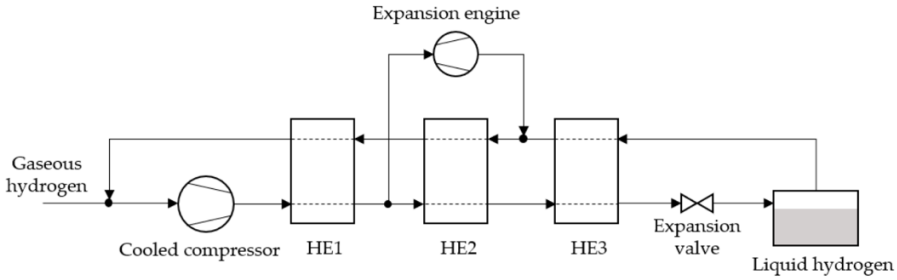

Figure 4: Flowsheet of a baseline hydrogen liquefaction cycle [19].

1.3.3 Chemical carriers

The physical storage methods discussed so far represent only a fraction of the technologies currently available. This brief overview is intentional, as the core of this thesis concerns hydrogen storage via chemical carriers. The following section therefore provides a detailed analysis of these energy carriers — with a particular focus on methanol, LOHC and ammonia — assessing their potential for large-scale transport and distribution.

1.3.3.1 Methanol

Among chemical carriers, *methanol* plays a leading role due to its high energy density and ease of handling. With a hydrogen storage capacity of 12.5% by weight and a volumetric density of approximately 99 kg/m^3, methanol represents a highly efficient solution for the high-density storage and transport of hydrogen in a stable liquid form.

The process functions as a closed cycle: hydrogen is initially "charged" through the hydrogenation of CO_2, a reaction where carbon dioxide and hydrogen combine to form methanol and water:

$$CO_2 + 3H_2 \leftrightarrow CH_3OH + H_2O$$

The primary advantage of this carrier lies in the fact that methanol is a stable liquid under ambient conditions, which eliminates the evaporation losses (*boil-off*) typical of cryogenic systems and enables the use of existing logistical infrastructure, such as ships, tankers, and pipelines.

Regarding the hydrogen release phase (*dehydrogenation*), the most efficient technology is Methanol Steam Reforming (MSR), this process is governed by the same chemical equation mentioned above. This reaction, which operates at relatively moderate temperatures between 230°C and 330°C, allows for the extraction of three moles of hydrogen for every mole of methanol (as can be seen from the stoichiometry of the equation) by utilizing the contribution of water in the process. An innovative aspect for overall efficiency is the possibility of directly

storing a methanol-water mixture; this simplifies the plant configuration and avoids the energy costs associated with the distillation of pure methanol [20].

1.3.3.2 Liquid Organic Hydrogen Carriers

Hydrogen can be stored and transported using Liquid Organic Hydrogen Carriers (LOHC). This storage concept is based on a reversible chemical cycle where a liquid medium is "loaded" with hydrogen during production and subsequently "discharged" (dehydrogenated) when the energy is required by the end-user [21].

The core of LOHC technology lies in two distinct thermodynamic processes that govern the transformation of the carrier [22]:

i. Hydrogenation (*Loading*): This is an exothermic reaction where the organic storage liquid is mixed with raw hydrogen in a reactor. Under the influence of a catalyst and specific temperatures, unsaturated chemical bonds are transformed into saturated ones, forming the corresponding saturated hydride, referred to as the "hydrogen carrier" (H_x-LOHC) [14, 26]. From a chemical equilibrium perspective, low temperatures and high pressures are the most favourable conditions for this phase.
ii. Dehydrogenation (*Unloading*): As the opposite of the hydrogenation process, dehydrogenation behaves as an endothermic reaction. In the presence of a catalyst, hydrogen is extracted from the H_x-LOHCs, making the hydrogen available for use and restoring the original carrier for a new cycle.

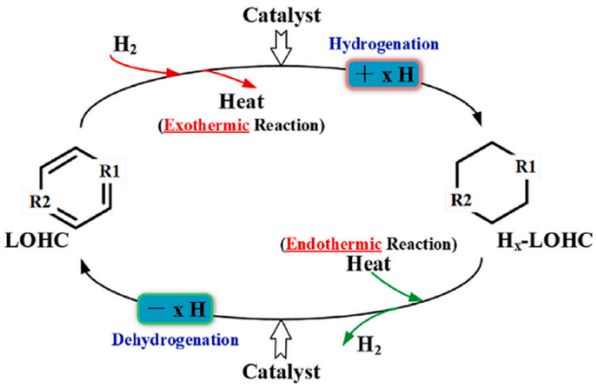

Figure 5: Hydrogenation-dehydrogenation process of the LOHCs technology [24].

The use of LOHCs offers a unique set of physical and economic advantages that address the primary challenges of hydrogen logistics. By significantly enhancing both volumetric and gravimetric storage capacities, the hydrogenation process theoretically enables long-term energy storage while eliminating the risks of leakage, boil-off, or other typical hydrogen losses associated with cryogenic systems [23, 25].

Beyond storage stability, ideal LOHCs are exceptionally easy to manage; they are safe, non-toxic, and remain in a liquid state under ambient conditions. This stability allows the hydrogen release process to be coupled with available low-temperature waste heat sources, thereby optimizing the overall thermal efficiency of the system. Furthermore, due to their physical properties being like those of crude oil derivatives, LOHCs can be transported and stored using existing infrastructure—such as tankers, terminals, and pipelines—requiring only minimal modifications to the current energy supply chain. One disadvantage of LOHCs is that, unlike ammonia, which can be converted simply by cracking, they require a continuous cycle of hydrogenation and dehydrogenation, increasing the complexity of the process.

Extensive research indicates that LOHC systems can be economically superior to both Compressed Hydrogen and Liquid Hydrogen transport systems, particularly for large-scale and long-distance distribution applications [25].

1.3.3.3 Ammonia as hydrogen carrier

The role of ammonia as a hydrogen storage carrier is supported by thermodynamic and physical properties that are superior to competing solutions. As highlighted in the study by Hasan et al. [24], ammonia exhibits the highest gravimetric and volumetric densities among a wide range of materials (as shown in Figure 6), establishing itself as an optimal storage solution in terms of efficiency and capacity.

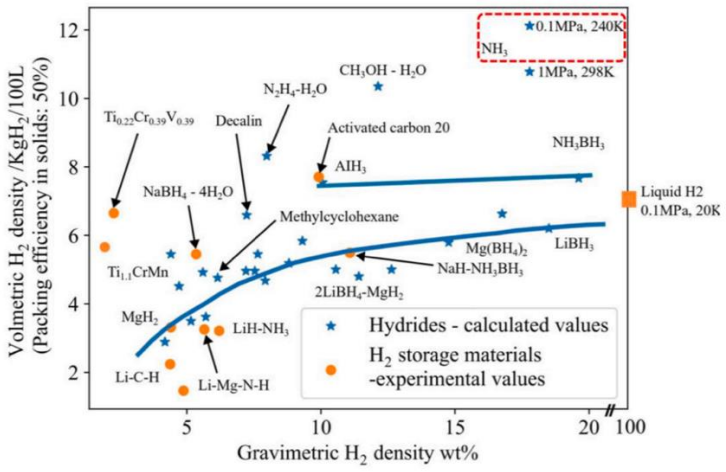

Figure 6: The gravimetric density of H_2 in its various energy carriers [25].

Ammonia (NH_3) has thus established itself as a key technology in the hydrogen-based energy system, thanks to these excellent chemical and physical properties. From an energy density perspective, liquid ammonia boasts a volumetric capacity of 121 kg_{H_2}/m^3 and a gravimetric density of 17.8% by weight. While this energy density is approximately half that of gasoline, it exceeds that of common batteries by more than tenfold [26].

The technical characteristics that make ammonia an efficient energy carrier have already been discussed; for greater clarity, we summarize them briefly [27]:

i. *Storage Conditions*: Ammonia can be maintained in the liquid phase at relatively moderate temperatures (-33 °C) at atmospheric pressure, or under pressure (less than 2 MPa) at ambient temperature. These conditions allow for fluid management that is significantly less complex than systems requiring extreme cryogenic temperatures.
ii. *Pipeline Transport*: Long-distance transport is achieved using carbon steel pipelines, a well-established technology. To cover a distance of 1610 km, the system requires an energy input of only 1119 kJ/kg_{H_2}. This efficiency is due to the nature of the fluid, which is moved in a liquid state with the aid of pumps.
iii. Regarding safety and sustainability, ammonia contains no carbon atoms, thus avoiding the production of pollutants such as CO or CO_2. While toxic at high concentrations, it's very low odor threshold (10-20 ppm [28]) serves as a natural safety indicator. Finally, ammonia offers unique versatility, as it can be used directly as a clean fuel in various industrial applications.

Based on the analysis of the various hydrogen storage technologies, it is evident that each carrier offers specific advantages and unique operational challenges. To provide a comprehensive overview and facilitate a direct comparison, Table [1] summarizes the key technical and performance parameters of the systems analysed. Specifically, a comparison is presented between compressed gaseous hydrogen (CGH_2), liquid hydrogen (LH_2), methylcyclohexane (MCH)—as a representative of liquid organic hydrogen carriers (LOHC)—and ammonia (NH_3).

Table 1: Comparison of H_2 storage options [28].

Properties	CGH_2	LH_2	MCH	Liquid NH_3	Methanol
Density (kg/m^3)	39	70.8	769	600	790
Storage pressure (MPa)	70	0.1	0.1	0.99	1
Storage temperature (°C)	25	-253	25	25	25
Gravimetric H_2 density (wt%)	100	100	6.2	17.8	12.5
Volumetric H_2 density (kg_{H_2}/m^3)	42.2	70.8	47.3	121	99

In conclusion, the comparative analysis highlights that the choice of a hydrogen carrier is strictly dependent on the specific requirements of the end-use application. While compressed and liquid hydrogen remain established solutions for direct, small-scale use, chemical carriers such as LOHCs and ammonia emerge as superior alternatives for long-haul transport and seasonal storage.

Ammonia stands out for its optimal balance between energy density and logistical ease, supported by a mature global infrastructure. Methanol is also a promising carrier due to its relatively simple handling, but its main limitation is that its oxidation releases CO_2, limiting its environmental sustainability. Although LOHCs (such as MCH) offer advantages in terms of safety and long-term stability, the energy requirements for dehydrogenation and their lower gravimetric density still pose significant challenges for large-scale adoption. In light of these considerations, this thesis focuses on the use of ammonia as the main energy carrier for optimising the hydrogen value chain.

Chapter 2

Ammonia Cracking Fundamentals: A comprehensive study on kinetics, catalysis, and advanced heating solutions.

Ammonia (NH_3), as stated in the previous chapter, has been recognized as a premier energy vector; however, the transition to a functional hydrogen-based economy is strictly dependent on the efficiency of its regeneration. This process, known as ammonia cracking, represents the most critical stage of the entire supply chain. As an endothermic catalytic reaction, the decomposition of NH_3 typically requires operating temperatures between 400°C and 700°C. While ammonia synthesis via the Haber-Bosch process is a long-standing and mature industrial technology, the on-site decomposition of NH_3 for energy applications remains a rapidly evolving field.

The hydrogen recovery process from ammonia is characterized by a five-stage value chain, as depicted in Figure 7. Current technologies for ammonia storage and transport (Step 01), along with hydrogen compression and end-use (Steps 04 and 05), are fully mature and commercially deployed. In contrast, the intermediate stages—specifically ammonia decomposition (cracking) and hydrogen purification (Steps 02 and 03)—currently constitute a significant technical bottleneck and are the primary focus of contemporary research [28].

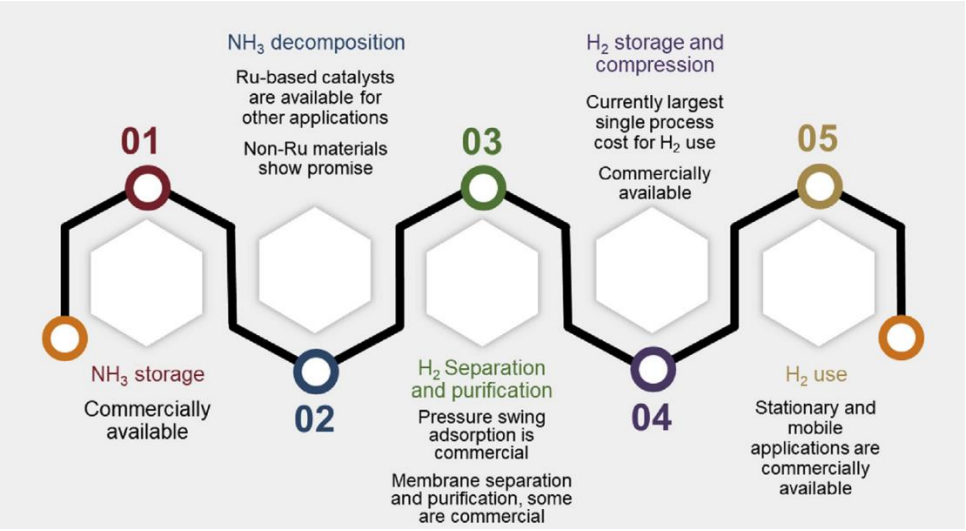

Figure 7: The five phases of power production from stored ammonia-derived hydrogen [29].

2.1 Thermodynamics and Kinetics of Ammonia Decomposition

The catalytic decomposition of ammonia is the reverse reaction of the Haber-Bosch synthesis and is represented by the following equilibrium:

$$2NH_3 \leftrightarrow N_2 + 3H_2 \qquad \Delta H = 91.2\ \frac{kJ}{mol}$$

From a thermodynamic perspective, this reaction is highly endothermic and requires temperatures generally ranging from 500 °C to 700 °C to proceed effectively [30]. While decomposition is theoretically possible at 698 K (425 °C), the reaction rate remains extremely slow without adequate thermal input and catalytic support. According to Le Chatelier's principle, the increase in moles (from 2 to 4) makes the process favoured by low pressures and high temperatures. Under normal atmospheric pressure, equilibrium conversions exceeding 99% are achieved only above 400 °C [32].

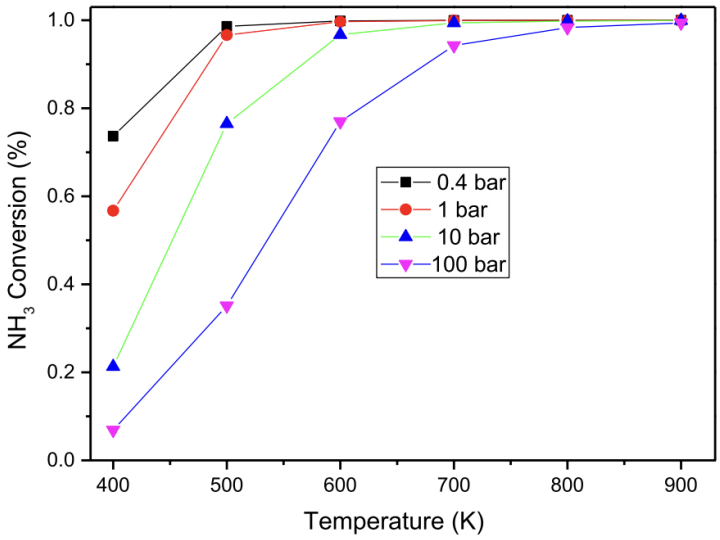

Figure 8: Equilibrium ammonia conversion depends on temperature at different pressures [31].

While thermodynamics defines the equilibrium limits, the kinetics of ammonia decomposition is governed by the interaction between NH_3 molecules and the catalyst surface. Although numerous catalyst alternatives exist, the fundamental decomposition process generally follows a sequence of surface-mediated steps. The standard model involves the initial adsorption of NH_3 onto an empty active site (*), followed by the progressive activation and cleavage of N-H bonds:

1. $NH_{3\,(g)} + * \leftrightarrow NH_{3\,(ads)}$
2. $NH_{3\,(ads)} + * \leftrightarrow NH_{2\,(ads)} + H_{(ads)}$
3. $NH_{2\,(ads)} + * \leftrightarrow NH_{(ads)} + H_{(ads)}$
4. $NH_{(ads)} \leftrightarrow N_{(ads)} + H_{(ads)}$
5. $2N_{(ads)} \leftrightarrow N_{2\,(g)} + 2*$
6. $2H_{(ads)} \leftrightarrow H_{(g)} + 2*$

The evolution of the above reactions can be illustrated with an image for greater clarity.

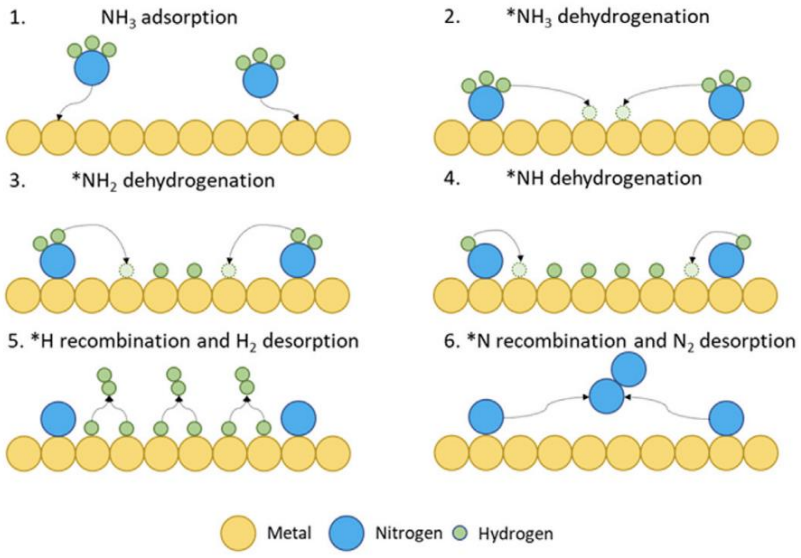

Figure 9: General reaction pathway for ammonia decomposition [32].

2.1.1 The Temkin-Pyzhev kinetic model

Most existing models for ammonia decomposition are based on the *Temkin-Pyzhev equation,* which is suitable for both NH_3 synthesis and decomposition. The reaction rate (r) is generally expressed as:

$$r = k_{app}\left[\left(\frac{p_{NH_3}^2}{p_{H_2}^3}\right)^{\beta} - \frac{p_{N_2}}{K_{eq}^2}\left(\frac{p_{H_2}^3}{p_{NH_3}^2}\right)^{1-\beta}\right]$$

Equation 1: Temkin-Pyzhev kinetic model [33].

In this model, the first term represents the ammonia decomposition rate, while the second term accounts for the contribution of the reverse (synthesis) reaction. However, in the high-temperature range of 673 to 1023 K, the second term is virtually zero, indicating that the reaction is not limited by equilibrium and the reverse reaction can be neglected [34].

The apparent reaction rate constant (k_{app}) follows the Arrhenius equation:

$$k_{app} = k_{0,app} \exp\left(\frac{E_{app}}{RT}\right)$$

Where k_{app} is the pre-exponential factor (dependent on metal loading), E_{app} is the apparent activation energy, and ß is the reaction order. Both ß and E_{app} are strongly dependent on the specific metal used.

Crucially, the rate-determining step (RDS) depends on the nature of the catalyst [37].:

i. For noble metals (e.g., Ru, Rh), the cleavage of the N–H bond is the RDS.
ii. For non-noble metals (e.g., Fe, Co, Ni), the desorption of N_2 becomes the RDS.

The transition from theoretical kinetics to practical simulation requires a clear distinction between intrinsic chemical properties and physical reactor parameters. As established in the literature, while the apparent activation energy (E_{app}) and the reaction order (ß) depend primarily on the active metal; the pre-exponential factor ($k_{0,app}$) must be adjusted based on the specific catalyst loading and dispersion on the binder [35].

Consistent with this approach, the Temkin-Pyzhev equation was selected as the kinetic model for the simulations conducted in Aspen Plus. This choice allows for a robust integration of the chemical kinetics within the software environment, providing a solid foundation for the reactor design. The model was implemented using the following kinetic parameters:

Table 2: Kinetic parameters used for the Temkin-Pyzhev equation in Aspen Plus simulations [36].

Apparent activation energy (E_{app})	120,000 kJ/kmol
Apparent pre-exponential factor ($K_{0,app}$):	$1{,}2 \cdot 10^9$ kmol/(m³·s)
ß coefficient	0.5

2.2 Catalysts for Ammonia Cracking

This part discusses the state-of-the-art of different catalysts utilized in this application. The discussion is further split into two major sections: the former section deals with Ruthenium-based (Ru) catalysts, which is the standard of high performance at this point in time based on their best nitrogen binding energy; the second section deals with Beyond-Ru catalysts. The analysis of the most promising industrial and commercial alternatives will be done in this latter part with particular attention to Nickel (Ni) and Iron (Fe) catalysts.

2.2.1 Ruthenium-based Catalysts (Ru)

Ruthenium (Ru), due to its overall superior activity for ammonia decomposition, is the most extensively studied monometallic catalyst for this reaction. Experimental data and computational studies have found that Ru is the most active among pure metals and thus is the benchmark for hydrogen production via NH_3 cracking.

The fundamental reason for this performance is that Ru is located closest to the peak of the Volcano Plot for ammonia decomposition, exhibiting an optimal nitrogen binding energy (N_2).

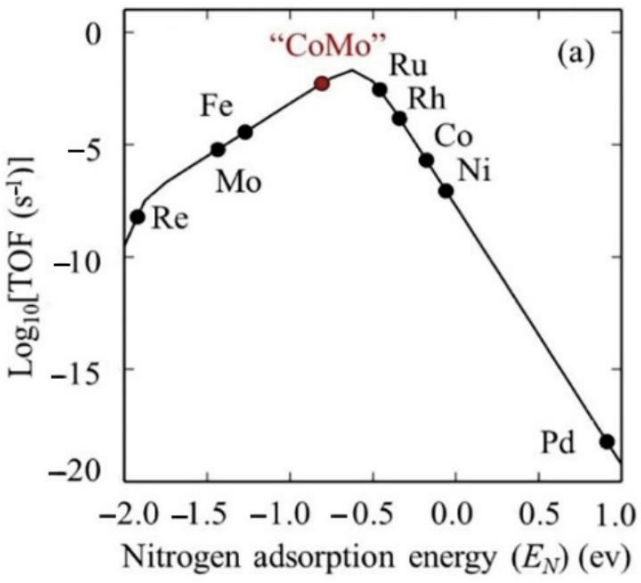

Figure 10: Turnover frequency (TOF) as a function of nitrogen adsorption [36].

The catalytic activity, as shown in the figure above, is dependent on the strength by which the metal surface adsorbs the nitrogen atoms. According to the Sabatier principle, an ideal catalyst must find a balance [37]:

- The binding energy must be high enough to facilitate the dissociation of the N-H bonds.
- It must be weak enough to permit the associative desorption of nitrogen (N_2) from the surface.

In contrast, metals such as Nickel (Ni) bind nitrogen too weakly to effectively initiate the reaction, while others like Iron (Fe) bind it too strongly, leading to surface saturation.

Beyond its intrinsic activity, an important advantage of Ru-based catalysts is their ability to operate under relatively low-temperature conditions.

However, the high cost of Ruthenium is the major factor that prevents widespread industrial use of the element. In order to solve this problem, two strategies have been studied:

- Total substitution of Ru with less expensive metals.
- Minimization of metal loading through maximization of Ruthenium dispersion on the support.

In this context, building of single-atom catalysts (SACs) has received a considerable impetus. This approach aims to expose the maximum number of active sites, specifically B-5 type sites (atomic steps on the Ru surface), which have been identified as the most active for NH_3 cleavage.

To be used on the industrial scale, these catalysts must resolve the challenges of low yield, high costs, labour-intensive manufacture processes, and low thermal stability [34].

2.2.2 Catalysts Beyond Ruthenium

To address the high cost and scarcity of noble metals, research has focused on developing catalysts based on more economical and stable transition metals, such as nickel (Ni), cobalt (Co) and iron (Fe). Among these, cobalt has been identified as a promising candidate to replace ruthenium, thanks to its favourable nitrogen adsorption properties and significantly lower cost.

However, replacing Ru with other metals (e.g. Co, Ni, Fe, Cr or their alloys) changes the operating conditions required. It has been observed that, when using these non-precious catalysts, high temperatures and low pressures are essential to achieve high-purity H_2 production.

Among such catalysts, nickel-based ones have proven to be very efficient non-Ru alternatives. Nevertheless, experimental findings [40] have shown that their activity is strongly affected by the support employed, i.e. the properties of the support material have a strong impact on the efficiency of ammonia decomposition.

One of the most important issues in Ni-based catalysis is the relationship between particle size, catalytic activity and turnover frequency (TOF). Decomposition of NH_3 on nickel is very morphology sensitive, whereby the particles exhibiting an average size of less than 2.9 nm are very active with an optimum size of 2.3 nm [38]. Beyond this nanometric scale, the catalyst efficiency is likely to decrease dramatically. This also underscores the importance of choosing those supports which can sustain high dispersion in metals and avoid formation of nickel crystallites (sintering) throughout the operation process which will otherwise impair the overall operation of the entire system.

Moreover, catalyst preparation procedure and metal loading are known to have a considerable impact on the ultimate performance. It has been proposed in comparative study that co-precipitation and adsorption techniques yield more active catalysts than the usual impregnation techniques, primarily because the dispersion and the size of the resulting nickel particles are improved.

Another economical substitute to noble metals is iron (Fe). Historically, early studies on the use of iron for ammonia decomposition were not focused on hydrogen production, but on the removal of NH_3 from hot exhaust gases during coal gasification [42]. The catalysis of iron is more complicated than that of ruthenium because iron is capable of forming stable nitride with ammonia. Research has shown that the formation of surface nitrides (Fe_xN) can greatly lower the rate of ammonia combustion and catalytic activity is also conditioned by iron phases [43]. Furthermore, high operating temperatures cause iron sintering, which can be prevented by using iron-based core-shell catalysts.

To summarize, a nickel (Ni)-based catalyst is chosen in this thesis based on literature review, with consideration of the cost, industrial availability and performance balance. This choice is consistent with industrial standards for the simulation of large-scale processes in the Aspen Plus environment, where nickel is the benchmark in terms of efficiency and economic feasibility.

2.3 Reactor configurations

After the selection of the catalytic system, the design of the reactor is the key element in ensuring that the heat required for the endothermic reaction is provided efficiently. Various configurations have been studied to optimize ammonia cracking, mainly differing in the heat transfer method and catalytic bed arrangement.

The most popular ones are packed-bed (PBR) ones, which keep the thermodynamic equilibrium unchanged; membrane reactors, which move the equilibrium by dissociating hydrogen; and microchannel reactors, which have a big surface-to-volume ratio.

2.3.1 Packed-bed reactors

One of the most popular configurations of the heterogeneous catalytic reactions in the field of chemical engineering are fixed bed reactors (PBRs). They are comprised of a cylindrical reactor containing a bed of solid catalytic particles, held in a fixed position, through which the reactant gas stream continuously flows. In this system, contact between the fluid phase and the solid phase occurs throughout the catalytic bed, allowing the desired chemical transformation to take place and be controlled.

Even though the fixed-bed reactors are commonly employed in industry, there are various imperative challenges related to them when utilized in highly endothermic processes, including the ammonia cracking process examined in the current study.

The first limitation is thermodynamic in nature: since the reaction is limited by equilibrium, the simultaneous presence of reactants and products within the same reaction volume imposes an intrinsic limit on the maximum conversion that can be achieved. The second dimension is the heat management. The static configuration of the catalytic bed favours the formation of temperature gradients along the reactor axis. In an endothermic process such as ammonia decomposition, this can result in the presence of areas with insufficient temperature, leading to a reduction in reaction rate and overall performance. Last, another critical problem is potential deactivation of the catalyst. During ammonia cracking, the hydrogen generated may adsorb on the active sites competitively to the adsorption of NH_3 and decreases the catalyst activity. This is especially applicable to catalysts that are prone to being poisoned by hydrogen.

To mitigate the critical issues typical of conventional fixed bed reactors (PBRs), multi-tubular configurations or multiple catalytic beds are frequently used. These plant solutions are designed to improve thermal control and reduce the effects of the limitations imposed by thermodynamic equilibrium, which in traditional systems can compromise process efficiency.

One such representative is the FTR technology, which was developed based on the traditional reformers in the case of methane reforming in steam. Here the reactor is a compartment of vertical tubes; they are crowded with a catalyst that is put inside them and fitted into a combustion chamber whereby the required heat is provided mainly by the radiation.

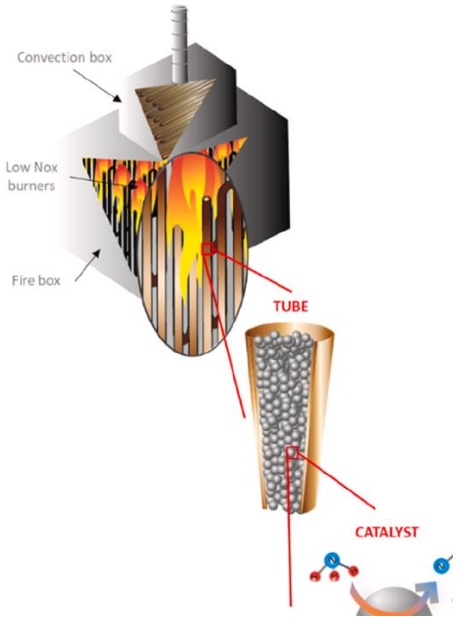

Figure 11: TFR technology [38].

Drawing on this well-established industrial technology, the tubular reactor ensures high reliability in supplying the energy required for the endothermic decomposition of ammonia. This configuration effectively minimizes the development of "cold spots" and ensures uniform heat distribution throughout the catalytic bed.

2.3.2 Packed–bed membrane reactors (PBMR)

Membrane reactors (MR) are innovative systems that combine chemical reaction and product separation in a single step. This integration simplifies the plant, reducing investment costs and energy consumption. The main advantage is the continuous extraction of hydrogen: by removing it as it forms, the product is prevented from accumulating on the surface of the catalyst and, according to Le Chatelier's principle, the reaction is driven to convert more ammonia than would normally be possible.

One of the simplest configurations to design and manage is the fixed bed (packed bed) membrane reactor. In this scheme, a bed of catalytic particles is placed in direct contact with one side of the membrane. Usually, the catalyst is located on the high-pressure side, while the low-pressure side collects the gas that passes through the membrane (permeate).

The design of these units depends on the arrangement of the catalyst and the direction of gas flow, leading to two main architectures:

- Internal Configuration: the membrane is deposited on the inner surface of the support and the catalyst surrounds it, promoting a flow that moves from the inside to the outside.
- External configuration: the membrane covers the outside of the support, and the catalyst is positioned outside, causing the gas to flow towards the inside of the unit.

Despite its simplicity, the fixed bed has some disadvantages, such as excessive pressure drops. Since hydrogen separation is driven by pressure, excessive leakage reduces the efficiency of the membrane. To limit this problem, larger catalyst particles are used, but this reduces the amount of catalyst available per unit area of the membrane [39].

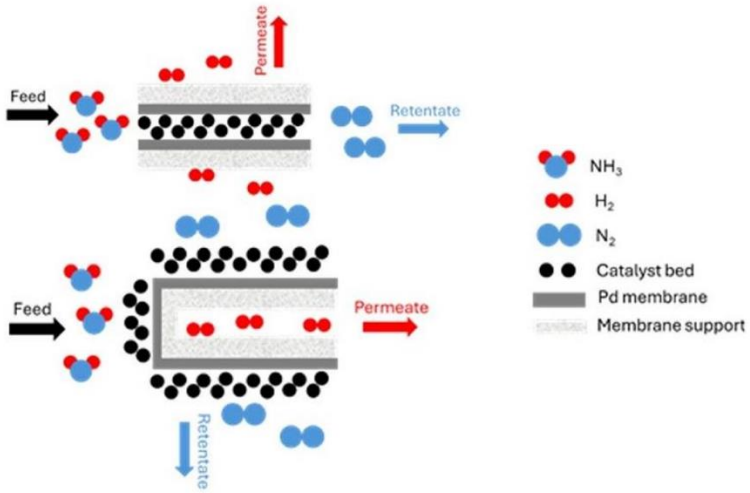

Figure 12: Schematic representation of the membrane reactor; (top) internal and (bottom) external packed bed configurations [35].

The reactor operates by constantly generating two separate flows: the permeate, i.e. the gas (typically hydrogen) that has passed through the membrane, and the retentate, which includes everything that remains in the reaction compartment.

The driving force behind this separation is the partial pressure gradient of hydrogen between the two sides of the membrane. To create the thrust necessary for the gas to pass through, the total pressure difference or the concentration of the species is usually adjusted. In more advanced configurations, this movement can also be facilitated by electrical or ionic gradients.

2.3.3 Catalytic Membrane Reactors (CMR)

Catalytic Membrane Reactors (CMRs) represent a further step forward in process intensification. Unlike traditional models, CMRs integrate a catalytic layer directly with a permeoselective membrane. This architecture has been specifically designed to overcome the transport limitations typical of fixed bed reactors and to maximise performance in ammonia decomposition.

CMRs allow immediate extraction of hydrogen as soon as it is generated. This approach offers several advantages:

- Thermal control: direct contact between the catalyst and the membrane improves heat exchange, ensuring more uniform temperature distribution. This homogeneity is essential for endothermic reactions such as ammonia cracking, as it improves both reaction kinetics and product selectivity.
- Product recovery: the close proximity of the components reduces diffusion limitations, increasing the overall efficiency of the system [35,46].

Scientific research has explored various solutions to optimise these devices. Some studies have focused on the use of thin layers of palladium (Pd) membranes deposited on a porous support. In particular, one effective technique involves depositing the selective layer directly in the mesoporous zone of the support, ensuring greater structural stability and clearer gas separation [38].

2.3.4 Microreactors and plasma-based technologies

The evolution of chemical engineering today sees the convergence between the structural precision of microreactors and the energy efficiency of plasma. This combination allows complex reactions, such as ammonia NH_3 cracking.

In practical terms, a plasma system consists of two key components that work together:

- The Plasma Generator: Uses electrical energy to ionise the gas, creating a highly active state of matter.
- The Reactor: This is the environment in which the plasma triggers and sustains radical chain reactions, transforming the reactants into products through high-energy molecular collisions [40].

The added value of plasma technology consists in the use of electrons as “activation carriers”. These are capable of exciting gas molecules and generating highly reactive chemical species. This mechanism allows highly endothermic reactions (which require heat), such as ammonia cracking (NH_3), to be carried out under much less harsh operating conditions than traditional techniques [41].

In the field of engineering, there are two types of plasma technologies:

- Thermal Plasma: This is defined as a state of thermodynamic equilibrium; all components (electrons, ions and neutral particles) share the same high temperature.
- Non-Thermal Plasma (NTP): This is characterised by a marked non-equilibrium. In this state, only electrons (which are very light) reach extremely high temperatures, while ions and neutral molecules remain at temperatures close to ambient temperature.

In non-thermal systems, ammonia decomposition occurs at significantly lower overall temperatures than in traditional thermochemical reactors [42]. The process is driven by high-energy electrons which, when colliding with ammonia molecules, transfer kinetic energy directly to the molecular bonds, thus triggering the cracking reaction through an electronic activation mechanism.

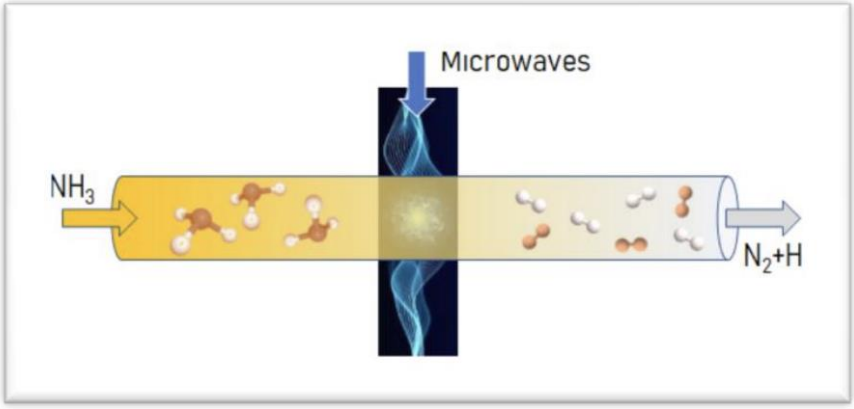

Figure 13: Schematic representation of a Microwave Plasma Reactor for ammonia decomposition. The diagram illustrates the conversion of NH_3 into N_2 and H_2 through a plasma zone generated by microwave radiation [42].

2.3.5: Heating methodologies analyzed in this thesis

The two central methodologies that are studied in this thesis in providing the energy required to conduct the endothermic cracking reaction of ammonia are:

- Thermal Heating: Examined as the conventional method, which is founded on combustion or the traditional radiant method.
- Electric Heating: Investigates the application of electrified technologies like resistive, induction or microwave heating.

Overall, the benefits of electric heating are manifold, and such requirements as the small reactor size, homogeneous heating, and exceeding controllability in the process are possible [42].

Resistive heating is one of the electrified technologies in which electric furnaces, heating bars or heating cylinders are used to convert electrical energy into heat. This method enables accurate control of material temperature and in addition, it is very efficient in the transfer of heat. In particular, direct Joule heating enables the provision of heat to the catalyst (and specifically to the catalytic sites) directly, avoiding any thermal constraints, and having a more precise control of the reaction front.

Electric induction heating, however, is founded on the relation between a time-varying magnetic field of high frequency and a conductor or ferromagnetic substance. This electromagnetic pressure causes eddy currents (or Foucault currents) in the material, and in the case of ferromagnetic materials, the unceasing repolarisation of the magnetic domains. Magnetic energy conversion to heat is consequently possible in two primary dissipating processes: the Joule effect which is associated with the electrical resistance of the material and magnetic hysteresis.

Both systems (electrical and thermal heating) were analyzed with the purpose of finding the most efficient and practical variant.

Chapter 3

Modelling and Simulation of the Ammonia Cracking Process in Aspen Plus

The plant design was developed to convert liquid ammonia to a high purity stream of hydrogen by an integrated and thermally efficient process. The working cycle starts by withdrawing liquid ammonia out of a storage tank which is at low temperature conditions or moderate pressure conditions. Before feeding the core of the system, the fluid must be processed through a feed and thermal integration section; here, the ammonia is vaporized and brought to the operating temperature by exploiting the heat recovered from the hot streams exiting the reactor. The whole cycle is based on this internal heat exchange, which is the primary cycle efficiency, since it significantly lowers the amount of external energy needed to preheat the feed.

When the optimum conditions are achieved the gaseous ammonia is passed through the catalytic decomposition reactor. In this stage, the cracking of the molecule takes place, splitting into hydrogen and nitrogen through a strongly endothermic reaction that requires a constant supply of thermal energy to be sustained. This section design is the key point of the current study since it is in this part that various heating strategies, including electrical to traditional combustion, are implemented and compared.

The gaseous stream exiting the reactor, consisting of the produced hydrogen and nitrogen mixture and a small fraction of unconverted residual ammonia, is then conveyed to the purification and finishing section. By a series of selective separation processes, impurities and nitrogen are eliminated to separate a final hydrogen stream at over 99.9% purity.

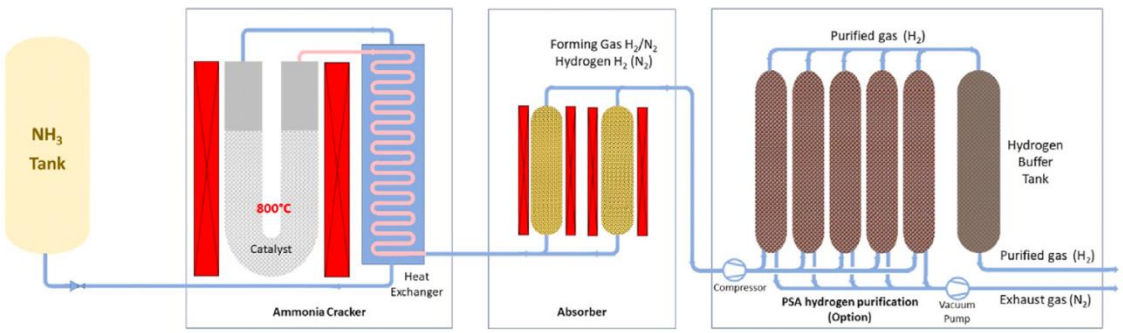

Figure 14: Schematic diagram of ammonia cracking process [43].

The implementation of a system based on the process architecture above was done in the Aspen Plus simulation environment. This is a starting point process specification whereby 38 tonnes of ammonia per day are introduced into the system to produce 5 tonnes of hydrogen per day.

The initial building block of the flowsheet was to choose the thermodynamic model, which is an essential task to make sure the software correctly computes the physical-chemical properties and enthalpy changes of the system.

3.1 Thermodynamic foundations of the simulation: ELECNRTL and Peng Robinson

The simulation of the hydrogen production process via ammonia cracking requires a hybrid thermodynamic approach. The need to model both high temperature gaseous reactions and chemical separation processes in the liquid phase resulted in the choice of two main frameworks in Aspen Plus: the Peng-Robinson equation of state (PR), and the ELECNRTL model.

The global property model of the simulation was the ELECNRTL (Electrolyte Non-Random Two-Liquid). This option is vital in the modelling of the absorption section where ammonia that remains is extracted through the application of acid scrubbing using sulfuric acid (H_2SO_4). ELECNRTL is an activity coefficient model designed specifically for non-ideal liquid systems containing ionic species. Unlike standard molecular models, it provides a rigorous description of the liquid phase through two primary contributions:

- Activity Coefficient Calculation: The model is accurate in calculating liquid-phase non-ideality by accounting not only the long-range forces between ions by electrostatic forces but also the short-range forces between charged and neutral species controlled by molecular interactions.
- Vapor Phase Description: In this model, an Equation of State is incorporated which is used to compute the fugacities and enthalpies of components in the gas phase.

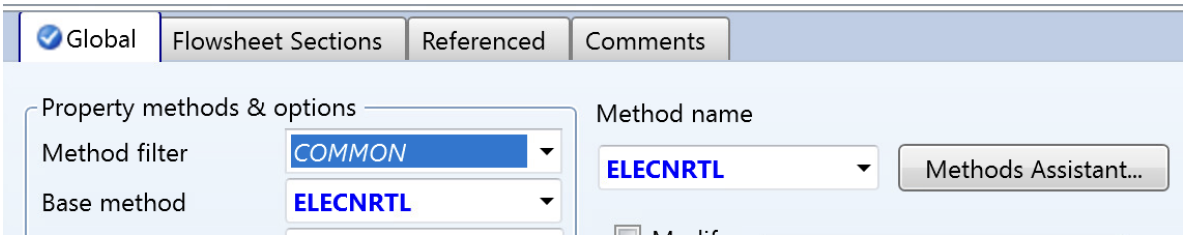

Figure 15: Selection of the ELECNRTL property method in Aspen Plus for thermodynamic property estimation.

In this section of the simulation environment, the Henry components have been defined. These are the species of the chemical which are in the supercritical state or the ones which are highly volatile in comparison to the main solvent (in this case, it is water). Unlike condensable components, their solubility in the liquid phase is not determined by standard equations of state but by application of Henry Law which is a relationship between the solute fugacity and solute molar fraction in the liquid phase based on a given, temperature-dependent constant.

In particular, the light gases/volatile solutes contained in the system (NH_3, N_2, H_2) were declared as Henry Components in order to properly model their solubility in the liquid phase, using the Henry constants that were incorporated in the Aspen Plus® database.

While ELECNRTL governs the electrolytic sections, the Peng–Robinson (PR) equation of state was utilized for the high-temperature cracking and gas-dominant sections of the plant. Being a cubic equation of state, it gives an accurate mathematical expression of the relationship between pressure, volume, and temperature:

$$P = \frac{RT}{v - b} - \frac{a(T)}{v(v + b) + b(v - b)}$$

The presence of PR model, Peng and Robinson, guarantees:

- Gas Phase Accuracy**:** Reliable calculation of thermodynamic properties (enthalpy, density, and fugacity) for the H_2, N_2, and NH_3 mixture at reaction conditions.
- Phase Equilibrium: Accurate prediction of the Vapor-Liquid Equilibrium (VLE) of non-polar and low polarity components in each of the different flash stages of the hydrogen loop.

3.2 Process Configuration: From Single Unit Operations to Integrated Flowsheet Design

3.2.1 Reactors and Intermediate Heating

The first section of the process focuses on ammonia conversion through a two-stage reaction configuration with intermediate heating. Figure 16 below illustrates that the feed stream (NH3FEED) is first heated in the HE1 heat exchanger. In order to maximize the total thermal efficiency and minimize the energy waste, the pre-heating stage uses the recovered heat of downstream process streams which reduces the requirement of external utilities.

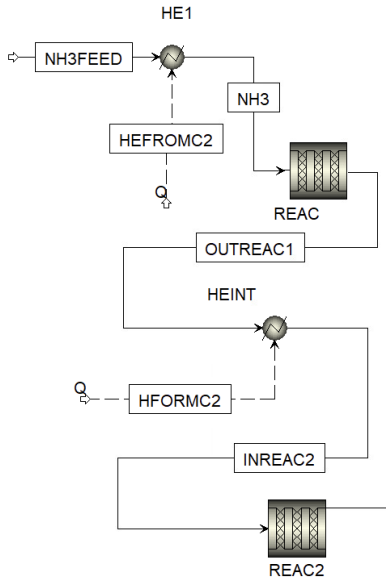

Figure 16: Flowsheet: Reaction section with cracking stages and intermediate heating.

Table 3: Plug Flow Reactor (PFR) design parameters.

Length [m]	2
Tube diameter [mm]	50
Number of tubes in each reactor	15
Catalyst loading (each reactor) [kg]	2
Bed voidage	0.4

At 220 °C, the ammonia enters the first reactor (REAC), in which the principal catalytic cracking reaction occurs. Because the cracking reaction is highly endothermic, it causes a temperature decrease along the catalyst bed. To counter the effect of this, an intermediate heating stage (HEINT) is introduced. This inter-stage heat is an important technique, with several benefits:

- Thermal Maintenance: It sustains high temperatures throughout the process, favouring reaction kinetics.
- Enhanced Conversion: It facilitates increased total conversion rates which would be impractical to accomplish in a single stage without too much thermal gradients.
- Optimized Heat Duty: It avoids the concentration of excessive heat duty in one vessel. This can be justified by the fact that the data presented in Figure 17 indicate that the heat delivered to a two-reactor system can be more efficiently distributed than the heat delivered to a single-reactor one.

The units are the Plug Flow Reactors (PFR), and the design parameter is presented in Table 3. The model used in the simulation is Temkin-Pyzhev kinetic model. The amount of heat duty supplied to each reactor is known and constant such that a total of 92% of the ammonia is converted at the outlet of the second reactor (REAC2).

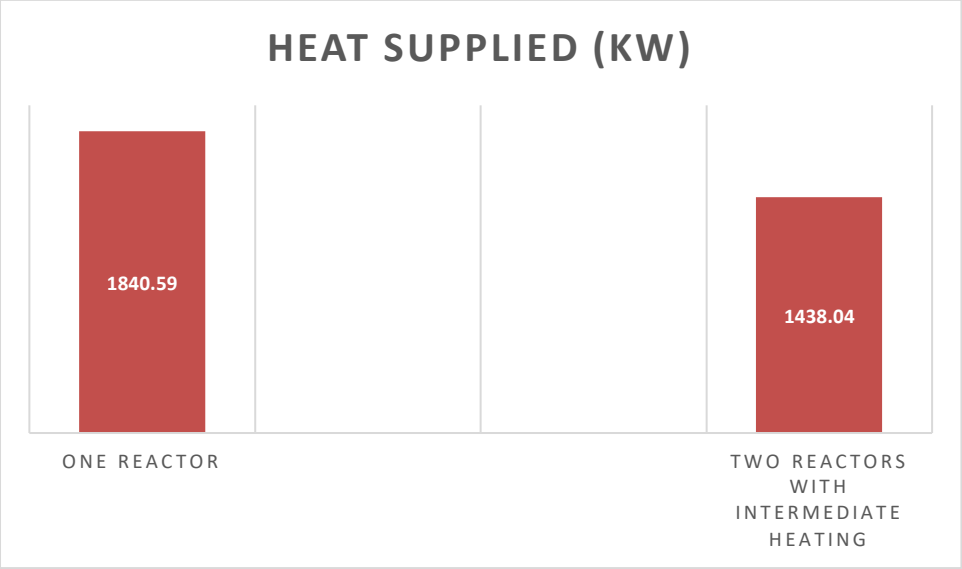

Figure 17: Comparison of total heat supplied: single reactor setup (left) vs two-reactor system with intermediate heating (right).

3.2.2 Reactor Sensitivity Analysis

To optimize the cracking process performance, a sensitivity analysis was conducted, focusing on the key operating variables of the PFR reactors. The research gives an insight into the direct impact of temperature changes and reactor geometry on reaction kinetics and resulting degree of conversion.

The relationship between the operating temperature and conversion of ammonia is depicted in Figure 18. The analysis shows an upward trend in that with increase in temperature there is an increase in the conversion but in the same direction in a near linear manner to about 445°C of both reactors after which it tends to asymptotically approach unity.

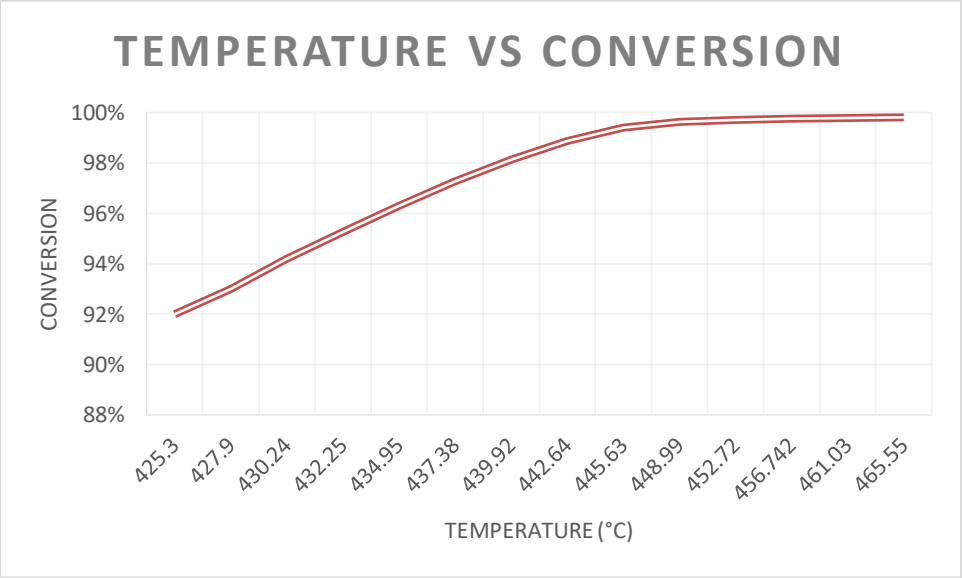

Figure 18: Ammonia conversion as a function of operating temperature.

Figure 19 illustrates the outcomes of the sensitivity analysis of the first reactor (REAC1). The aim of the study is to assess how the variation in reactor length (expressed in metres) affects the conversion of ammonia at the outlet.

Looking at the graph, we note that the conversion grows exponentially in the initial few metres and then levels off to a unit value with length. In this context, the choice of a length of 2 metres — the value actually set in the Aspen Plus simulator which also coincides with the optimal length of the second reactor— proves to be ideal, as it allows a significant degree of initial conversion to be achieved without exceeding the reactor dimensions, thus representing the best trade-off between thermochemical efficiency and size of the unit.

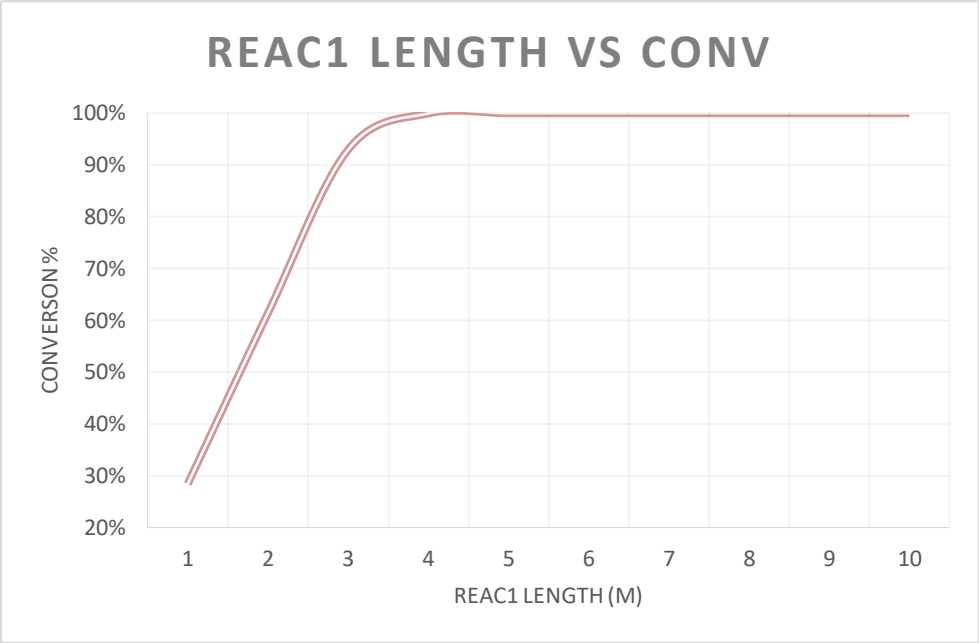

Figure 19: Conversion profile as a function of reactor length for REAC1.

3.2.3 Absorption and Stripping Section: Ammonia Recovery and Solvent Regeneration

To provide the general view of the purification system, Figure 20 presents the process flowsheet, with the stripping and absorption sections depicted in more detail, referring to the interconnections of the two units as well as to the solvent recycle loop.

The effluent exiting the second reactor undergoes a purification process to remove residual ammonia traces. As the cracking reaction occurs at atmospheric pressure, the gas stream is initially compressed to 19 atm and cooled to 100 °C.

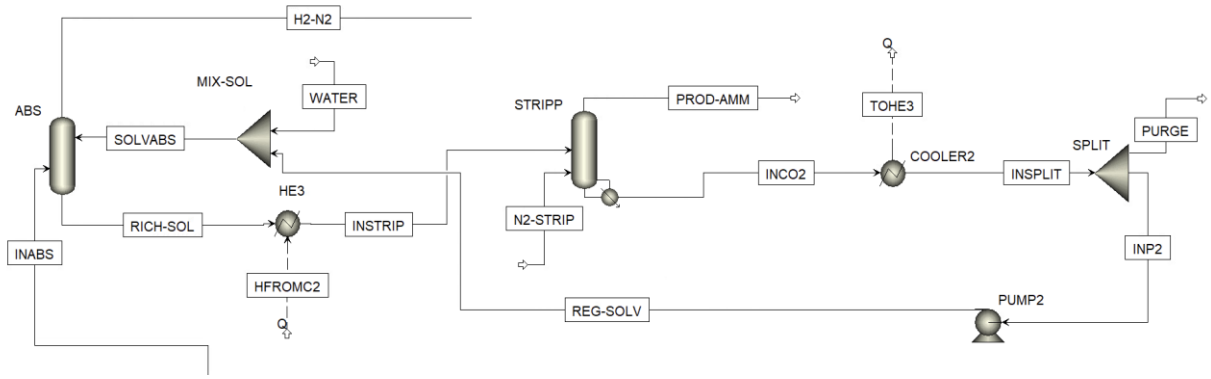

Figure 20: Process flow diagram of the ammonia absorption and stripping section.

The cooled and compressed gas is then pumped into an absorption column, technical specifications of which are explained in Table 4. A solution of water and sulfuric acid (H_2SO_4) is fed counter-currently from the top of the column. The use of sulfuric acid is a strategic choice: the formation of ionic species facilitates the chemical binding of ammonia, drastically improving its solubility in water and ensuring its efficient removal from the gas phase.

The top of the absorber contains a purified gas stream, consisting almost entirely of hydrogen and nitrogen, with the ammonia mass fraction reduced to approximately $8{,}38 \cdot 10^{-7}$. The liquid bottom stream, containing water and the chemically bound ammonia, is directed to a stripping column. The primary objective of this unit is to regenerate the solvent solution, which is then recycled back to the top of the absorber to complete the solvent loop.

Table 4: Operating parameters for the absorption column.

Number of stages	15
Pressure [atm]	19
Condenser	None
Reboiler	None
Absorber efficiency [%]	99

The stream of liquid at the bottom of the absorber (RICH-SOL) containing the ammonia chemically bound to the acidic solution is sent to the regeneration part. The stream then flows through a heat exchanger (HE3) in which the temperature of the stream is raised with the recovery of heat in process streams (HFROMC2), thereby improving the separation capacity.

The stripping of ammonia is carried out in a column (the column specifications are presented in Table 6) with the stripping agent of nitrogen (N_2). The latter is fed into the base of the column at a mass flow rate of 1 kg/h. The nitrogen stream enhances extraction of ammonia between the liquid and the gas phase; as such, the top of the stripper produces PROD-AMM stream with a recovery of ammonia of about 3 tons per day and an input of ammonia of 38 tonnes per day.

A sensitivity analysis was conducted on the number of equilibrium stages in the stripper. Specifically, the stages were adjusted differentially depending on the ammonia concentration in INCO2 stream. The results showed that increasing the number of stages led to a progressive

reduction of ammonia in INSTRIP resulting in significantly cleaner water. However, a higher number of stages also implies increased capital costs for the column. Therefore, the final number of stages was selected as a compromise between separation performance and equipment cost.

Table 5: Sensitivity analysis, number of stages was varied as a function of the ammonia content in the INCO2 stream.

Number of stages	Mass flow of ammonia in INSTRIP [kg/hr]
18	$3{,}68 \cdot 10^{-11}$
20	$1{,}44 \cdot 10^{-12}$
22	$5{,}62 \cdot 10^{-14}$
25	$4{,}34 \cdot 10^{-16}$

The regenerated solvent (REG-SOLV) is recovered at the bottom of the stripper, showing a negligible ammonia mass fraction ($6{,}19 \cdot 10^{-15}$). The solution mainly made of water and regenerated sulfuric acid is cooled down in COOLER2 to an optimum temperature of working in the absorption stage. Finally, the stream enters a split unit (SPLIT): a small portion is removed as PURGE in order to help eliminate the accumulation of inert species, while the main fraction is directed to the pump (PUMP2) and recycled back into the absorption loop, ensuring the continuous reuse of the sulfuric acid solution.

Table 6: Operating parameters for the stripping column.

Number of stages	22
Pressure [atm]	1
Condenser	None
Reboiler	Kettle
Stripping agent	N_2

Absorption is preferable at low temperatures and maximum ammonia separation by stripping is possible only at high temperatures; therefore, a heat exchanger (HE3) is inserted between the two units. This component acts as a thermal interface, heating the RICH-SOL stream exiting the absorber before it enters the stripper, thereby optimizing the overall performance of the recovery loop.

3.2.4 Hydrogen Purification: Pressure Swing Adsorption (PSA) Section

The final stage of the purification process involves separating hydrogen from the gas mixture exiting the absorber. In the simulation, the Pressure Swing Adsorption (PSA) section was modelled using a simplified separator block.

The primary objective of the overall process—the production of high-purity hydrogen—is successfully achieved: the PSA unit yields approximately 5 tons per day of hydrogen from the top stream, with a purity of 99.9%. Regarding separation efficiency, the simulation results show that 90.6% of the inlet hydrogen is successfully recovered in the H_2 stream, while the remaining 9.4% is lost in the N_2 waste stream.

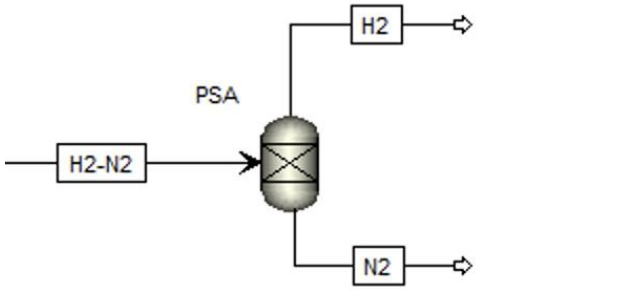

Figure 21: PSA section.

3.3 Global Flowsheet

Ultimately, Figure 22 presents the comprehensive plant flowsheet. Within the simulation, all thermal integrations have been optimized to maximize energy recovery and minimize waste. Specifically, the heat streams exiting the cooling units indicate that excess thermal energy is

not dissipated but rather recovered and repurposed in other sections of the plant where heat input is required (incoming streams), thus ensuring high overall cycle efficiency.

Regarding the global mass balance, the plant is fed with 38 tons per day of ammonia. Following the cracking, absorption, and PSA purification stages, a final output of 5 tons per day of high-purity hydrogen is achieved, fully meeting the established production targets.

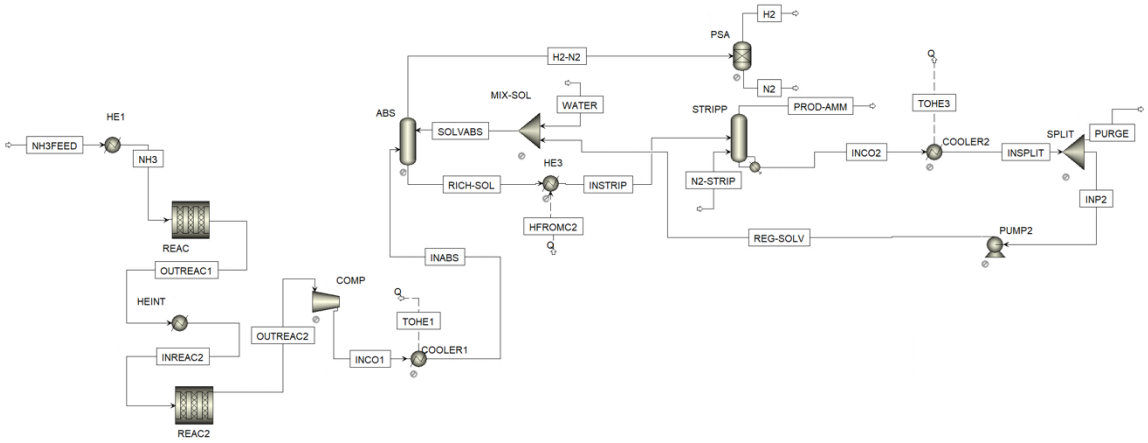

Figure 22: Comprehensive process flowsheet implemented in Aspen Plus®.

Chapter 4

H_2 and NH_3 as Green Fuels for the Ammonia Cracking Process

The current chapter seeks to examine the thermal supply strategies in detail that is needed to support the highly endothermic nature of the ammonia cracking reaction. Despite the growing focus on industrial electrification as a decarbonization strategy, combustion remains the primary solution for high-heat-demand industries, if zero-carbon energy carriers are used.

In this context, three main configurations for fuelling the reactor burner were investigated:

- Hydrogen Combustion: use a portion of the generated hydrogen.
- Ammonia Combustion**:** the recovery of the residual ammonia stream (designated as PROD-AMM in Figure 22). This stream is not thrown away or even vented but rather celebrated as a fuel which enhances the overall effectiveness of the plant.
- Ammonia/Hydrogen Blend Combustion: a hybrid solution aimed at balancing the ignition properties of hydrogen with the energy density of ammonia.

The flammability limits were evaluated for all three scenarios described above, in order to ensure that the operating conditions always remain within the flammability triangle and to guarantee process safety. Lastly, according to Aspen Plus simulation software, quantitative analysis of the formation of nitrogen oxide (NO_x) was done keeping track of the environmental impact of each of the solutions to determine the best trade-off between energy efficiency and the containment of the polluting emissions.

4.1 Hydrogen Combustion

Hydrogen has the potential to play a crucial role in the global energy transition as a versatile and carbon-free energy carrier. When utilized in combustion processes or fuel cells, hydrogen reacts with oxygen to produce water as the primary byproduct. This feature leads to a small environmental footprint and essentially zero greenhouse gas (GHG) emissions [44] which makes it a perfect choice to make high-temperature industrial processes like ammonia cracking decarbonized.

The management of hydrogen, however, should be done with due caution to its reactivity. Hydrogen-oxidant mixtures are flammable, and their flammability limits depend on several factors, including:

i. Ignition energy and temperature.
ii. Operating pressure.
iii. The presence of diluents.
iv. The specific geometry and dimensions of the combustion equipment.

In order to provide safety of operations, hydrogen mixtures may be diluted with innocuous constituents up to the point when the concentration is less than the Lower Flammability Limit (LFL). The notable feature of hydrogen is the extremely broad range of its flammability in the atmosphere, ranging between 4 % and 75 % in volume. This is significantly broader than that of methane (4.3-15% vol) or gasoline (1.4-7.6% vol). Also, the energy needed to start ignition is exceptionally small; hydrogen needs just 0.02 mJ, which is almost an order of magnitude below that needed by methane (0.28 mJ), or gasoline (0.24 mJ)[44].

4.1.1 Modelling and Flammability Analysis of H_2 Combustion in Aspen Plus

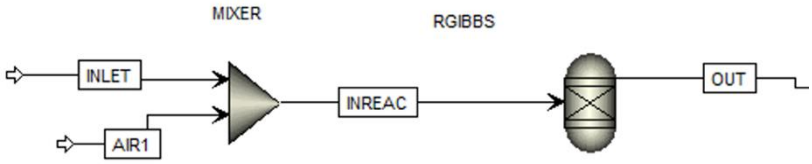

Figure 23: Aspen Plus combustion process flowsheet, reactant mixing and Gibbs reactor.

To evaluate the correctness and the safety considerations of heating section, the specific simulation was created in Aspen Plus as shown in flowsheet above. This processing is performed by employing in this setup a MIXER block that mixes the fuel stream (INLET) and the combustion air (AIR1); the mixture is then fed to an RGIBBS reactor to simulate the combustion process under thermodynamic equilibrium conditions.

The choice of RGIBBS reactor is especially suitable in this kind of analysis. Unlike other types of reactors, it does not need preset reaction stoichiometry or kinetic parameters. Instead, the outlet composition is determined by minimizing the total Gibbs free energy of the system, thereby identifying the equilibrium state at the specified temperature and pressure (atmospheric pressure and adiabatic reactor). This technique is particularly suitable to the determination of the formation of small species, like nitrogen oxides (NO_x), the concentration of which highly relies on the equilibrium situation that is formed in the flame.

The methodology adopted contained the following steps:

Data Acquisition: The information of Lower Flammability Limit (LFL) and Upper Flammability Limit (UFL) of hydrogen-air mixture [Table 7] was obtained in the literature [46].

Composition Calculation: The exact percentage of hydrogen in the INREAC stream (hydrogen + air mixture) was calculated using Aspen Plus.

Safety Verification: The percent obtained was assessed as compared to the flammability range. (This evaluation confirmed whether the mixture was flammable and suitable for sustaining combustion within the burner, while ensuring that operating conditions remained within established safety margins).

Based on the stoichiometric ratio of 34.29 kg_{air}/ kg_{H_2} required for complete combustion, the Aspen Plus simulation uses a hydrogen flow rate of 70 kg/h, with the air feed adjusted to maintain this 34.29 ratio.

Table 7: Flammability limits of hydrogen–air mixture at various initial temperatures [46].

Temperature °C	**LFL H_2-air**	**UFL H_2-air**
20	4.5	75.0
150	4.0	79.5
300	3.5	83.0
400	3.0	85.5

4.1.2 Simulation Results and Flue Gas Composition for Hydrogen Combustion

Based on the implemented model, the composition of the gas exiting the RGIBBS reactor was used to verify the achievement of thermodynamic equilibrium in the combustion process and, subsequently, to derive the values from which the concentrations of the pollutant species, expressed in parts per million (ppm), were determined.

Table 8: Composition of the outlet stream (OUT) and detail of NOx in ppm for hydrogen combustion.

Chemical species	Mole fractions	Concentration (ppm)
N_2	0,6534	-
H_2O	0,3457	-
O_2	0,00084	-
NO	$1{,}50 \cdot 10^{-6}$	1,50
NO_2	$6{,}01 \cdot 10^{-9}$	0,01

4.2 Ammonia Combustion

Even though ammonia (NH_3) is a promising energy carrier to decarbonize the energy sector, chemical and physical properties have challenging effects that severely hinder its use in practice compared to conventional fuels.

The primary weakness is the low reactivity of the molecule. Ammonia has an extremely low laminar flame speed, measured at approximately 0.07 m/s. To put this figure into context, consider that natural gas burns at a speed five times higher (0.37 m/s), while hydrogen reaches 2.91 m/s [45].The other obstacle is the adiabatic flame temperature that is approximately 1800 ° C. This value is significantly lower than that of methane (1950 °C) and hydrogen (2110 °C).

The most important issue is the local environmental impact. Although theoretical stoichiometric combustion does not produce nitrogen oxides, real operating conditions are always not perfect. The inherent content of nitrogen in the fuel encourages the development of intermediate radicals which encourage high NO_x emissions. The difficulty of maintaining the fine line between the necessity to stabilise the naturally slow flame and the necessity to minimise the creation of nitrogen pollutants is to date the most complicated engineering task of the to-be-adopted ammonia, on an industrial scale.

4.2.1 Modelling and Flammability Analysis of NH_3 Combustion in Aspen Plus

The ammonia combustion process implementation in the Aspen Plus environment is based on the identical logic architecture used in hydrogen (outlined in paragraph 4.1.1).

Table 9: Flammability limits of ammonia–air mixture at various initial temperatures [46].

Temperature °C	LFL NH_3-air	UFL NH_3-air
20	16.5	29.0
150	15	32.5
300	12.5	35.5
400	11.0	37.1
500	11.0	38.5

Similarly to hydrogen, the molar fraction of ammonia estimated by the simulation was considered, and the reactivity conditions were established by making sure that such a concentration was strictly within the restricted range of flammability characteristic of this molecule.

4.2.2 Simulation Results and Flue Gas Composition for Ammonia Combustion

Based on the results obtained from the model, the data relating to the molar fractions and concentrations of the pollutant species, expressed in parts per million (ppm), are summarised in the following table.

Based on the stoichiometric ratio of 6.06 kg_{air}/kg_{NH3} required for complete combustion, the Aspen Plus simulation uses an ammonia flow rate of 100 kg/h, with the air feed adjusted to maintain this 6.06 ratio.

Table 10: Composition of the outlet stream (OUT) and detail of NO_x in ppm for ammonia combustion.

Chemical species	Mole fractions	Concentration (ppm)
N_2	0,6891	-
H_2O	0,3104	-
O_2	0,0005	-
NO	$1{,}66 \cdot 10^{-5}$	16,58
NO_2	$9{,}47 \cdot 10^{-9}$	0,01

4.3 Ammonia-Hydrogen Combustion

During the recent years, there has been an increased interest among the scientific community in ammonia as an energy carrier. In this regard, the concept of mixing NH_3 with more reactive fuels being among the most successful options to offset its inherent constraints has steadily become more popular. Specifically, the mixture with highly reactive fuels has been observed to be one of the primary approaches to enhancing flame stability, in the conventional combustion systems that were initially designed to respond to traditional fuels.

In this perspective, the NH_3/H_2 mixture appears particularly interesting. Both components can be considered clean fuels, because, under conditions of complete combustion, they give rise to N_2 and H_2O, species that do not have any significant direct environmental effects [46].

Moreover, hydrogen is important in enhancing the behaviour of the mixture: its broad flammability range and high specific calorific value help to enhance the overall reactivity and stabilise the combustion process, which at least partially counteracts the critical concerns of ammonia.

Their interest in such blends is also not just theoretical but is translated into practical uses especially in the development of gas turbine (GT) systems. Herein, Yao et al. [46] have pointed to the possibility of using ammonia-hydrogen blends as a power source that does not emit carbon to power turbines. At the same time, they have shown that system performance is strongly influenced by the mixing ratio between the two fuels, a parameter that directly impact on the combustion behaviour and overall efficiency.

In the perspective of the basic burning parameters, Lee et al. [47] experimentally investigated the laminar flame velocity (LBV) of ammonia-hydrogen mixtures at atmospheric pressure (0.1 MPa). The results clearly show that as the hydrogen fraction increases, so does

the LBV: hydrogen compensates for the slow kinetics of pure ammonia, making the mixture more suitable for the residence times typical of industrial combustors.

Nevertheless, the problem of emissions is still unresolved. Although these blends have definite benefits in the form of stability of flames and the absence of carbon, the essential problem of factoring in the creation of nitrogen oxides (NO_x) remains the primary technological issue.

4.3.1 Modelling and Flammability Analysis of NH_3-H_2 Combustion in Aspen Plus

Regarding the simulation in the Aspen Plus environment, the model structure occurs under the same logical scheme already used in the analysis of the separate components, hydrogen and ammonia, that were introduced in the earlier sections. Basically, the fundamental set up has been preserved as a way of maintaining consistency in the results comparison.

The initial step in the characterisation of the mixture was the definition of the flammability limits (LFL and UFL) that are required to find out the appropriate operating range under safe conditions.

The procedure adopted was as follows:

- Lower Flammability Limit (LFL): To calculate the lower limit of the mixture, the rule of Le Chatelier was used, according to which the overall value can be determined by multiplying the molar fractions with the flammability limits of the individual components. The theoretical result was then compared with experimental data available in the literature (see Figure 24), showing good consistency under the considered process conditions, referring to the temperature of the reactor feed stream of 44 °C.
- Upper Flammability Limit (UFL): The upper limit was approached in a conservative manner. Instead of a weighted average, the most restrictive value associated with hydrogen (75.6%) was used. This figure was also advanced to 80 percent as a cautionary factor, to insert an added safety margin of the simulations.

The flammability parameters so ascertained and adopted in further simulations are: LFL H_2-NH_3 16,83 % and UFL H_2-NH_3 80 %.

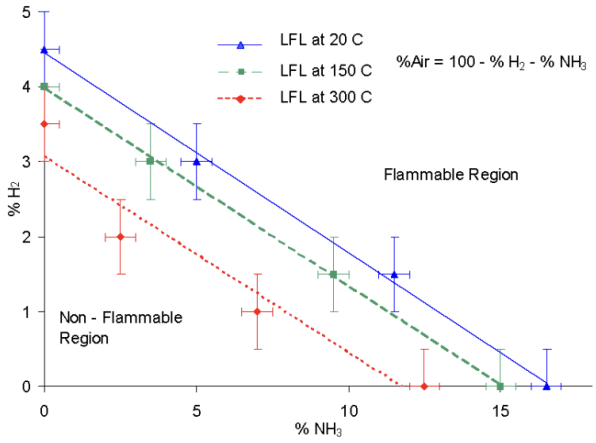

Figure 24: Effect of temperature and composition of the NH_3/H_2 mixture on the lower flammability limit (LFL) [47].

4.3.2 Simulation Results and Flue Gas Composition for Ammonia-Hydrogen Combustion

After having carried out the thermochemical modelling in Aspen Plus, the information concerning to the composition of the flow leaving the combustion reactor was extracted.

The concentration profiles obtained are presented in the table below: for the main species, the molar fraction is indicated, while for pollutants, the concentrations are expressed in parts per million (ppm) and in molar fractions.

Regarding the mixture inlet, an optimal equivalence ratio of 1.69 was maintained. Therefore, the initial mass flow rates for both hydrogen and ammonia were set at 100 kg/h each [44].

Table 11: Composition of the outlet stream (OUT) and detail of NOx in ppm for hydrogen-ammonia combustion.

Chemical species	Mole fractions	Concentration (ppm)
N_2	0,6660	-
H_2O	0,3022	-
O_2	$2{,}57 \cdot 10^{-13}$	-
NO	$3{,}69 \cdot 10^{-10}$	0,0004
NO_2	$3{,}46 \cdot 10^{-18}$	$3{,}46 \cdot 10^{-12}$

4.4 Conclusion: Decarbonisation Potential of H_2–NH_3 Combustion Systems

A comparison of the simulation results — considering the combustion of pure hydrogen, pure ammonia and their mixture — points out some remarkable differences in terms of environmental point of view.

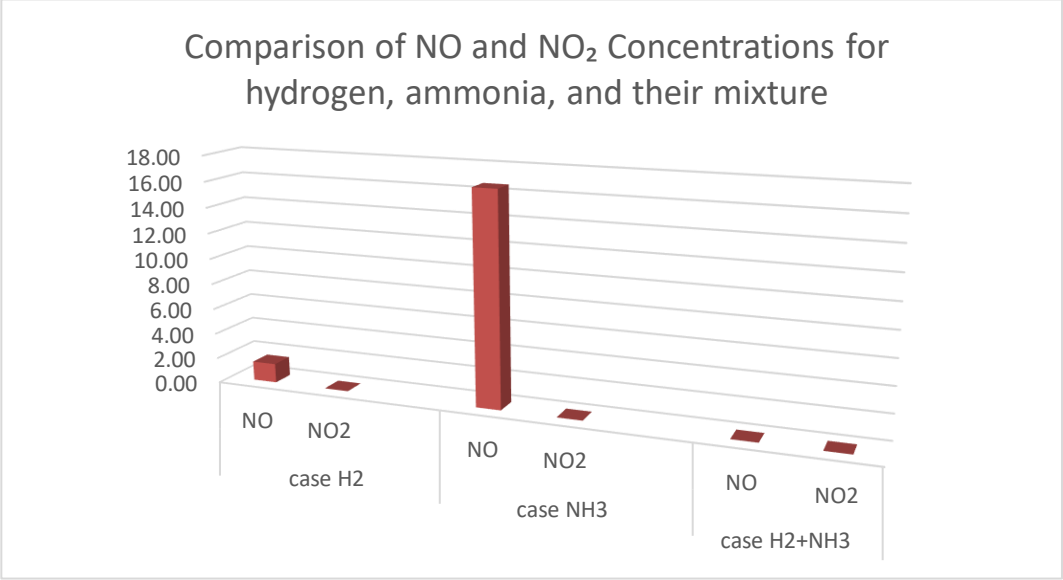

Figure 25: Comparison of NO and NO_2 Concentrations (ppm) for hydrogen, ammonia, and their mixture.

The attained concentration profiles reveal that NH_3/H_2 mixture has a tangible benefit in pollutant reduction: the concentrations of nitrogen oxides (NO_x), especially NO and NO_2, are lower than those associated with the utilization of one of the two pure fuels. This factor is one of the main factors in the general evaluation of the emission performance of the system.

This makes the hydrogen-ammonia blend a highly viable solution in the decarbonisation landscape. The efficiency of this mixture is not only based on a decrease of harmful emissions but also on the enhancement of the dynamic performance of the process. The literature confirms [45] that the addition of hydrogen acts as a real reaction promoter, substantially enhancing the stability of ammonia combustion.

To sum up, the synergy between the high reactivity of hydrogen and the intrinsic characteristic of ammonia makes it possible to overcome the kinetic limitations of the latter, while at the same time ensuring a lower emission profile and a more flexible and safer thermal control of the combustor.

Chapter 5

Economic analysis and evaluation of the Levelized Cost of Hydrogen (LCOH)

The goal of this final chapter is to determine the economic sustainability of the analyzed technological solutions by translating technical and thermodynamic parameters into comparable cost metrics. The core of the evaluation lies in the calculation of the Levelized Cost of Hydrogen (LCOH), a fundamental parameter that indicates how much it costs, in euros, to produce one kg of hydrogen.

The analysis was conducted by comparing the two main configurations of the thesis:

- Heating by classical combustion.
- Electric heating.

The cost structure has been separated into CAPEX (Capital Expenditure) and OPEX (Operating Expenditure) items which differ significantly with the heat input technology adopted.

In the classical combustion-based configuration, an intrinsic increase in OPEX is observed due to the need to thermally sustain the cracking reaction. To ensure the net output of 5 t/d (the aim of the following thesis work), it is in fact essential to provide a higher ammonia input (41 tons/day compared to the base value of 38 tons/day) than in the electrical case, since a fraction of the flow must be diverted towards the combustor to feed the process. This surplus of raw material increases variable costs and is inevitably also reflected in CAPEX: the need to manage higher mass flow rates requires a larger sizing of all equipment, to which must be added the cost of installing the furnace, a component that represents an exclusive expense item of this configuration.

Conversely, in the electric configuration, it is sufficient to consider the ammonia input of the base case, equal to 38 tons/day, while the operating costs (OPEX) must account for the amount of electricity required to power the reactor.

5.1 OPEX and CAPEX in Electric Heating

The cost analysis for configuring the electric heating system was divided into the evaluation of capital investments and annual operating costs.

The estimation of the annual operating costs was based on the following parameters:

- C_L (Operating Labor Cost): Staffing cost, calculated based on a staff of 6 units dedicated to plant management.
- C_{RM} (Cost of consumables): Include the cost of raw material; water and sulfuric acid (for the absorber), nitrogen used as a stripping agent in the stripper, nickel-based catalyst and ammonia input.
- C_U (Utilities Cost): Includes the electricity needed to power the compressors and provide heat to the two reactors *(The electricity price considered is 70 USD/MWh).*
- FCI (Fixed Capital Investment): Represents the sum of direct costs (purchase and installation) and indirect costs (construction expenses and legal, contingency, etc.)
- WCI (Working Capital Investment): Calculated as a function of the cost of purchasing equipment. The Equipment Purchase Cost of the main units (reactors, PSAs, heat exchangers and compressors) were estimated using literature formulas [48] dependent on the size and capacity of the plant.

In the scenario of electric heating to establish the overall cost of operation, the following formula was used *(the formula was taken from article [47]):*

$$OPEX = C_{RM} + 2{,}3125C_L + C_U + 0{,}125FCI + 0{,}1\,TCI$$

To calculate the annualized CAPEXs, the following operating parameters were considered:

- i (Discount Rate): Actuation rate, set at 0.1 (10%).
- n (Plant Life): Useful life of the plant, set at 25 years.
- TCI (Total Capital Investment): The total investment calculated as the sum of FCI and WCI.

The CRF, capital recovery factor, is the coefficient used to determine the uniform annual value of the investment (it is calculated using the standard financial formula [47]) and, following the methodology present in the literature, the annual investment quota (CAPEX) is then obtained by multiplying the capital recovery factor by the total investment.

$$CAPEX = CRF \cdot TCI$$

In this study, the values used are:

- $CRF = 0.11$, calculated for the given discount rate and plant life.
- $FCI = 8776456{,}97$ USD/year, representing the fixed capital investment.
- $WCI = 1549810{,}85$ USD/year, representing the working capital investment.

thus, the total capital investment (TCI) amounts to $8776456{,}97\ USD/year$.

Table 12: CAPEX and OPEX, electric heating.

CAPEX €/kg$_{H_2}$	964.990,41
OPEX €/kg$_{H_2}$	8375128,77

In order to determine the relative importance of the various economic elements in managing the plant, an analysis of the ratio between the annualized cost of investment (CAPEX) and the annualized cost of operation (OPEX) was conducted.

As illustrated in the graph below, the cost structure of the electric heating configuration is characterized by a strong predominance of capital-related expenses. The greatest part of the overall annual expenditure is related to recovery of the Total Capital Investment (TCI) that is primarily attributed to the high cost of major equipment, especially the PSA unit. Operating expenses (OPEX, approximately 10% of the total) constitute a comparatively smaller portion of the annual cost. These include expenditures for electrical utilities (C_U), labor (C_L), and raw materials (C_{RM}).

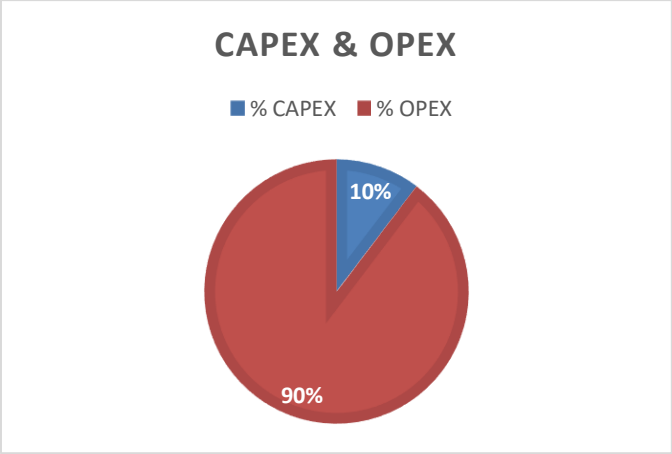

Figure 26: Distribution of total annual costs between CAPEX and OPEX for electrical heating.

5.2 OPEX and CAPEX in Combustion Heating

Similarly to that of the electric heating system, the case of the traditional combustion had the same economic estimation procedure applied. Although the methodological structure remains unchanged, significant variations are found in the main cost items.

As previously mentioned, the CAPEX and OPEX in this configuration are elevated due to the additional cost of purchasing the furnace, which significantly affects the Equipment Purchase Cost, as well as the increased operating costs resulting from the larger amount of ammonia required by the system. Below are the calculations for the two cost items:

In this study, the values used are:

- $CRF = 0.11$, calculated for the given discount rate and plant life.
- $FCI = 4749038{,}4\ USD/year$, representing the fixed capital investment.
- $WCI = 1930375{,}5\ USD/year$, representing the working capital investment.

  thus, the total capital investment (TCI) amounts to $12861940{,}2\ USD/year$.

Table 13: CAPEX and OPEX, combustion heating.

CAPEX €/kg$_{H_2}$	1201949,15
OPEX €/kg$_{H_2}$	10632722,99

The pie chart below shows the distribution of annual costs for this conventional thermal configuration. Compared to the electrical solution, it is noted that the increase in CAPEX was proportionally more marked than that of OPEX, occupying a significantly larger portion of the total.

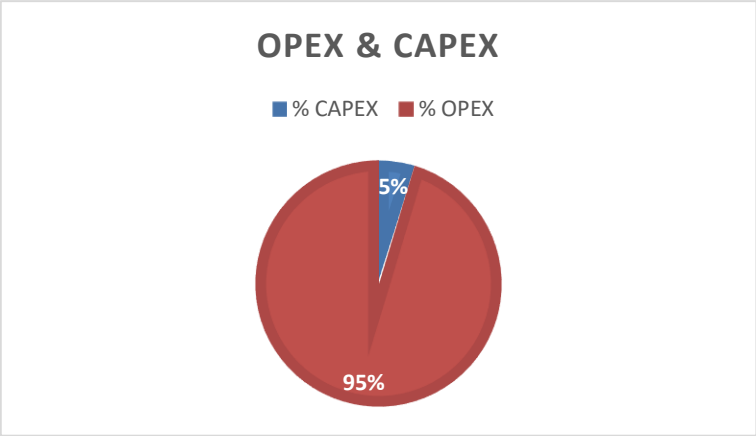

Figure 27: Distribution of total annual costs between CAPEX and OPEX for combustion heating.

5.3 Comparison between the two LCOHs

The Levelized Cost of Hydrogen (LCOH) is the basic measure of the economic sustainability of the project, which enables the two plant solutions examined to be compared directly.

The calculation was carried out by relating the sum of the investment costs (CAPEX) and operating costs (OPEX) accumulated over the entire life cycle of the plant to the overall quantity of hydrogen produced.

The values obtained for the two scenarios are as follows:

- Conventional combustion heating: 6,45 €/kg_{H_2}.
- Electrical Heating: 4,87 €/kg_{H_2}.

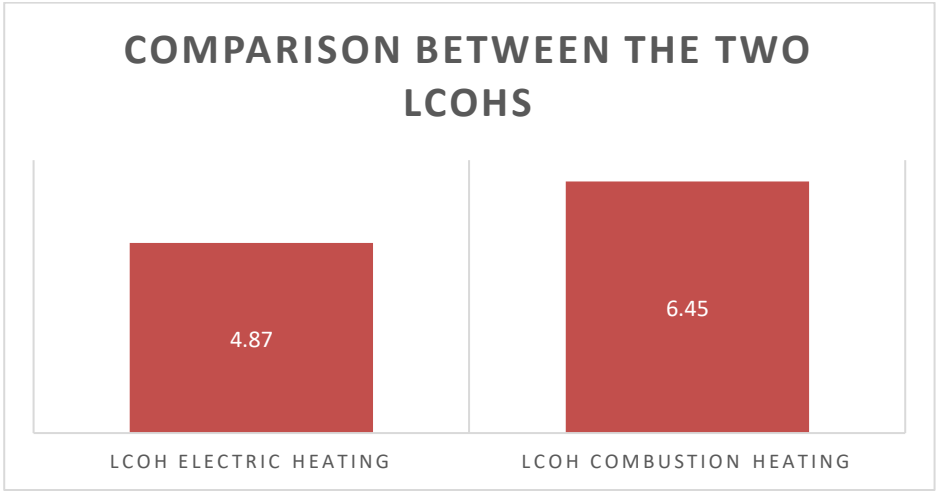

Figure 28: Comparison of LCOHs in €/kg_{H_2}.

5.4 Comparison with LCOH to produce hydrogen via fossil fuels

According to *Global Hydrogen Review 2025* [49], in 2022, gas prices, as a result of the war in Ukraine, increased dramatically. At that time, producing hydrogen from fossil fuels became so expensive (around \$9 per kg of H_2) that green hydrogen became competitive for the first time.

The main issue was that, at that moment, there were no green hydrogen production plants readily available to replace natural gas.

In the two years following 2024, the market experienced a significant decline in gas prices, bringing the cost of fossil-based hydrogen back down to very low levels, ranging between \$0.8-\$4 per kg of H_2. Meanwhile, the green hydrogen industry has been exposed to some new pressures: the cost of raw materials and components increased due to inflation, and the implementation of new technologies is slower than anticipated.

In this context, the results of the analysis offer an interesting point of reflection: hydrogen produced through combustion shows a cost slightly above €6/kg_{H_2} (around \$5/kg_{H_2}), while in the case of electric heating the LCOH drops to just over €4/kg_{H_2} (approximately \$4.2/kg_{H_2}). Considering that hydrogen from fossil sources ranges between \$0.8 and \$4/kg_{H_2}, the value obtained in the electric scenario suggests that, at least theoretically, green hydrogen production could already be positioned within a competitive economic range compared to conventional technologies.

Conclusion and future perspectives

The thesis was devoted to the modelling and implementation in Aspen Plus of an ammonia cracking process that is directed to the synthesis of green hydrogen, which is a very topical topic in the framework of global decarbonization and the transition from fossil fuels to renewable energy sources. In this scenario, hydrogen emerges as the key energy carrier for decoupling energy consumption from CO_2 emissions, surpassing the current industrial paradigm based on grey hydrogen, which, produced by reforming natural gas, generates a significant environmental impact of approximately 10 tons of carbon dioxide for every ton of hydrogen. Despite the fact that water electrolysis is the most adopted method of acquiring green hydrogen, the criticalities of storage and transportation are the significant technical restriction, which resulted to finding alternative solutions, including the use of ammonia as an energy carrier.

The analysis of two heat processes to the cracking reactor was the subject of study whereby, the traditional combustion process that entails the generation of pollutants like nitrogen oxides (NOx) was compared to the electric heating. It was shown that, if combustion were chosen, the most promising solution in terms of reducing the release of greenhouse gases and polluting species would be the use of hydrogen-ammonia mixture, but a detailed economic assessment that was integrated in analysis allowed outlining an even clearer picture.

The results relating to the calculation of the LCOH (Levelized Cost of Hydrogen) demonstrate that the configuration based on electric heating not only cancels emissions into the atmosphere but has lower production costs than the conventional route. Finally, it is concluded that ammonia cracking by electricity power is a better solution both in environmental perspective and economically and LCOH values are very competitive with the conventional production of fossil sources. These findings provide a strong basis to consider when creating new industrial projects to completely exclude the use of fossil fuels in the hydrogen supply chain and play a key role in meeting the climate goals established by 2050. It should nevertheless be considered that electric heating is strongly influenced by the cost of electricity, which represents one of the main economic variables of the process.

The outcomes achieved here lead to various insights that will be required in a subsequent shift to industrial scale. To begin with, the further evolution of the work will involve the optimization of the adsorption purification system: being in the current model Pressure Swing Adsorption (PSA) modelled as an ideal separator, a new analysis should involve the specific adsorption cycles or selective membranes elaboration. This detail is essential since hydrogen intended for fuel cells (Fuel Cells) requires extremely high purity and the energy required for these separation stages could significantly impact the final LCOH calculation.

Simultaneously, process validation will be subject to an in-depth investigation of the dynamics and intermittency of renewable sources. Since the electric heating supply must come from renewable sources such as solar and wind, it will be crucial to analyse how the cracking

reactor responds to changes in energy load and whether thermal storage systems are needed to ensure operational stability.

Economically, since electricity LCOH here is extremely sensitive to the kWh price, future research might map the comfort of the procedure across various geographical regions. It would be highly interesting to evaluate the competitiveness of the technology in markets with divergent costs of energy, such as in Italy, but in regions like North Africa or Chile, where the abundance of solar resources would be able to drastically lower the cost of production.

Finally, the transition from simulation in Aspen Plus to the construction of a pilot plant will require a scale-up study to address the construction challenges related to the strength of materials at high temperatures and the management of large-scale flows, fundamental steps to make ammonia cracking a consolidated reality.

Bibliography

[1] [Online]. Available: https://www.un.org/en/climatechange/net-zero-coalition.

[2] M. M. H. Bhuiyan and Z. Siddique, "Hydrogen as an alternative fuel: A comprehensive review of challenges and opportunities in production, storage, and transportation," *Int. J. Hydrog. Energy*, vol. 102, pp. 1026–1044, Feb. 2025, doi: 10.1016/j.ijhydene.2025.01.033.

[3] K. Mazloomi and C. Gomes, "Hydrogen as an energy carrier: Prospects and challenges," *Renew. Sustain. Energy Rev.*, vol. 16, no. 5, pp. 3024–3033, Jun. 2012, doi: 10.1016/j.rser.2012.02.028.

[4] K. Lee, X. Liu, P. Vyawahare, P. Sun, A. Elgowainy, and M. Wang, "Techno-economic performances and life cycle greenhouse gas emissions of various ammonia production pathways including conventional, carbon-capturing, nuclear-powered, and renewable production," *Green Chem.*, vol. 24, no. 12, pp. 4830–4844, 2022, doi: 10.1039/D2GC00843B.

[5] "Ammonia Technology Roadmap Towards more sustainable nitrogen fertiliser production." [Online]. Available: IEA (2021), Ammonia Technology Roadmap, IEA, Paris https://www.iea.org/reports/ammonia-technology-roadmap, Licence: CC BY 4.0

[6] C. Anand *et al.*, "Green hydrogen for a sustainable future: A review of production methods, innovations, and applications," *Int. J. Hydrog. Energy*, vol. 111, pp. 319–341, Mar. 2025, doi: 10.1016/j.ijhydene.2025.02.257.

[7] A. Valera-Medina, H. Xiao, M. Owen-Jones, W. I. F. David, and P. J. Bowen, "Ammonia for power," *Prog. Energy Combust. Sci.*, vol. 69, pp. 63–102, Nov. 2018, doi: 10.1016/j.pecs.2018.07.001.

[8] "Encyclopaedia Britannica Ammonia, chemical compound." [Online]. Available: https://www.britannica.com/science/ammonia

[9] "Karabeyoglu A, Brian E. Fuel conditioning system for ammonia fired power plants." [Online]. Available: https://nh3fuel.wordpress.com/wp-content/uploads/2012/10/evans-brian.pdf

[10] "Health and Safety Executive. EH40/2005 Workplace exposure limits, London." [Online]. Available: https://www.hse.gov.uk/pUbns/priced/eh40.pdf

[11] "Cole-Parmer Instrument Company. Chemical compatibility database, ammonia, anhydrous." [Online]. Available: https://www.coleparmer.co.uk/Chemical-Resistance

[12] "PHYSICAL AND CHEMICAL PROPERTIES OF HYDROGEN Isao Abe Office Tera, Chiba, Japan." [Online]. Available: https://www.eolss.net/sample-chapters/c08/e3-13-01-01.pdf

[13] A. A. Levikhin and A. A. Boryaev, "Physical properties and thermodynamic characteristics of hydrogen," *Heliyon*, vol. 10, no. 17, p. e36414, Sep. 2024, doi: 10.1016/j.heliyon.2024.e36414.

[14] N. D. Ngasse Moudio, X.-Q. Bian, and D. S. Chinamo, "Liquid hydrogen carriers for clean energy systems: A critical review of chemical hydrogen storage strategies," *Fuel*, vol. 404, p. 136329, Jan. 2026, doi: 10.1016/j.fuel.2025.136329.

[15] Y. Kojima and M. Yamaguchi, "Ammonia as a hydrogen energy carrier," *Int. J. Hydrog. Energy*, vol. 47, no. 54, pp. 22832–22839, Jun. 2022, doi: 10.1016/j.ijhydene.2022.05.096.

[16] M. Yang, R. Hunger, S. Berrettoni, B. Sprecher, and B. Wang, “A review of hydrogen storage and transport technologies,” *Clean Energy*, vol. 7, no. 1, pp. 190–216, Feb. 2023, doi: 10.1093/ce/zkad021.

[17] T. Zhang, J. Uratani, Y. Huang, L. Xu, S. Griffiths, and Y. Ding, “Hydrogen liquefaction and storage: Recent progress and perspectives,” *Renew. Sustain. Energy Rev.*, vol. 176, p. 113204, Apr. 2023, doi: 10.1016/j.rser.2023.113204.

[18] M. Niermann, S. Timmerberg, S. Drünert, and M. Kaltschmitt, “Liquid Organic Hydrogen Carriers and alternatives for international transport of renewable hydrogen,” *Renew. Sustain. Energy Rev.*, vol. 135, p. 110171, Jan. 2021, doi: 10.1016/j.rser.2020.110171.

[19] M. Aziz, “Liquid Hydrogen: A Review on Liquefaction, Storage, Transportation, and Safety,” *Energies*, vol. 14, no. 18, p. 5917, Sep. 2021, doi: 10.3390/en14185917.

[20] J. Andersson and S. Grönkvist, “Large-scale storage of hydrogen,” *Int. J. Hydrog. Energy*, vol. 44, no. 23, pp. 11901–11919, May 2019, doi: 10.1016/j.ijhydene.2019.03.063.

[21] M. Niermann, S. Timmerberg, S. Drünert, and M. Kaltschmitt, “Liquid Organic Hydrogen Carriers and alternatives for international transport of renewable hydrogen,” *Renew. Sustain. Energy Rev.*, vol. 135, p. 110171, Jan. 2021, doi: 10.1016/j.rser.2020.110171.

[22] C. Chu, K. Wu, B. Luo, Q. Cao, and H. Zhang, “Hydrogen storage by liquid organic hydrogen carriers: Catalyst, renewable carrier, and technology – A review,” *Carbon Resour. Convers.*, vol. 6, no. 4, pp. 334–351, Dec. 2023, doi: 10.1016/j.crcon.2023.03.007.

[23] M. Reuß, T. Grube, M. Robinius, P. Preuster, P. Wasserscheid, and D. Stolten, “Seasonal storage and alternative carriers: A flexible hydrogen supply chain model,” *Appl. Energy*, vol. 200, pp. 290–302, Aug. 2017, doi: 10.1016/j.apenergy.2017.05.050.

[24] M. H. Hasan *et al.*, “A Comprehensive Review on the Recent Development of Ammonia as a Renewable Energy Carrier,” *Energies*, vol. 14, no. 13, p. 3732, Jun. 2021, doi: 10.3390/en14133732.

[25] D. K. Madheswaran *et al.*, “Ammonia as a hydrogen carrier: A comprehensive analysis of electrolysis efficiency and its potential in sustainable energy systems,” *Renew. Sustain. Energy Rev.*, vol. 221, p. 115915, Oct. 2025, doi: 10.1016/j.rser.2025.115915.

[26] F. B. Juangsa, A. R. Irhamna, and M. Aziz, “Production of ammonia as potential hydrogen carrier: Review on thermochemical and electrochemical processes,” *Int. J. Hydrog. Energy*, vol. 46, no. 27, pp. 14455–14477, Apr. 2021, doi: 10.1016/j.ijhydene.2021.01.214.

[27] M. H. Hasan *et al.*, “A Comprehensive Review on the Recent Development of Ammonia as a Renewable Energy Carrier,” *Energies*, vol. 14, no. 13, p. 3732, Jun. 2021, doi: 10.3390/en14133732.

[28] K. E. Lamb, M. D. Dolan, and D. F. Kennedy, “Ammonia for hydrogen storage; A review of catalytic ammonia decomposition and hydrogen separation and purification,” *Int. J. Hydrog. Energy*, vol. 44, no. 7, pp. 3580–3593, Feb. 2019, doi: 10.1016/j.ijhydene.2018.12.024.

[29] A. S. Farooqi *et al.*, “A comprehensive review on hydrogen production via catalytic ammonia decomposition over Ni-based catalysts,” *Int. J. Hydrog. Energy*, vol. 97, pp. 593–613, Jan. 2025, doi: 10.1016/j.ijhydene.2024.11.357.

[30] S. R. Arsad *et al.*, “Patent landscape review of hydrogen production methods: Assessing technological updates and innovations,” *Int. J. Hydrog. Energy*, vol. 50, pp. 447–472, Jan. 2024, doi: 10.1016/j.ijhydene.2023.09.085.

[31] O. A. Ojelade and S. F. Zaman, “Ammonia decomposition for hydrogen production: a thermodynamic study,” *Chem. Pap.*, vol. 75, no. 1, pp. 57–65, Jan. 2021, doi: 10.1007/s11696-020-01278-z.

[32] N. Zecher-Freeman, H. Zong, P. Xie, and C. Wang, “Catalytic cracking of ammonia toward carbon-neutral liquid fuel,” *Curr. Opin. Green Sustain. Chem.*, vol. 44, p. 100860, Dec. 2023, doi: 10.1016/j.cogsc.2023.100860.

[33] D. Maccarrone *et al.*, “A Comprehensive Review on Hydrogen Production via Catalytic Ammonia Decomposition,” *Catalysts*, vol. 15, no. 9, p. 811, Aug. 2025, doi: 10.3390/catal15090811.

[34] S. Devkota *et al.*, “Process design and optimization of onsite hydrogen production from ammonia: Reactor design, energy saving and NOX control,” *Fuel*, vol. 342, p. 127879, Jun. 2023, doi: 10.1016/j.fuel.2023.127879.

[35] A. Di Carlo, L. Vecchione, and Z. Del Prete, “Ammonia decomposition over commercial Ru/Al2O3 catalyst: An experimental evaluation at different operative pressures and temperatures,” *Int. J. Hydrog. Energy*, vol. 39, no. 2, pp. 808–814, Jan. 2014, doi: 10.1016/j.ijhydene.2013.10.110.

[36] H. Yousefi Rizi and D. Shin, “Green Hydrogen Production Technologies from Ammonia Cracking,” *Energies*, vol. 15, no. 21, p. 8246, Nov. 2022, doi: 10.3390/en15218246.

[37] N. Zecher-Freeman, H. Zong, P. Xie, and C. Wang, “Catalytic cracking of ammonia toward carbon-neutral liquid fuel,” *Curr. Opin. Green Sustain. Chem.*, vol. 44, p. 100860, Dec. 2023, doi: 10.1016/j.cogsc.2023.100860.

[38] S. Richard, A. Ramirez Santos, P. Olivier, and F. Gallucci, “Techno-economic analysis of ammonia cracking for large scale power generation,” *Int. J. Hydrog. Energy*, vol. 71, pp. 571–587, Jun. 2024, doi: 10.1016/j.ijhydene.2024.05.308.

[39] F. Gallucci, “Packed bed membrane reactors,” in *Current Trends and Future Developments on (Bio)Membranes*, Elsevier, 2023, pp. 59–75. doi: 10.1016/B978-0-12-823659-8.00004-6.

[40] N. Li, C. Zhang, D. Li, W. Jiang, and F. Zhou, “Review of reactor systems for hydrogen production via ammonia decomposition,” *Chem. Eng. J.*, vol. 495, p. 153125, Sep. 2024, doi: 10.1016/j.cej.2024.153125.

[41] I. Fedirchyk, I. Tsonev, R. Quiroz Marnef, and A. Bogaerts, “Plasma-assisted NH3 cracking in warm plasma reactors for green H2 production,” *Chem. Eng. J.*, vol. 499, p. 155946, Nov. 2024, doi: 10.1016/j.cej.2024.155946.

[42] M. Awaji, L. Pentecoste-Cuynet, C. Noël, T. Gries, M. Belmahi, and T. Belmonte, “Ammonia cracking by microwave plasma under reduced pressure,” *Int. J. Hydrog. Energy*, vol. 119, pp. 377–385, Apr. 2025, doi: 10.1016/j.ijhydene.2025.03.118.

[43] K. Trangwachirachai, K. Rouwenhorst, L. Lefferts, and J. A. Faria Albanese, “Recent progress on ammonia cracking technologies for scalable hydrogen production,” *Curr. Opin. Green Sustain. Chem.*, vol. 49, p. 100945, Oct. 2024, doi: 10.1016/j.cogsc.2024.100945.

[44] C. B. B. Farias, R. C. S. Barreiros, M. F. Da Silva, A. A. Casazza, A. Converti, and L. A. Sarubbo, "Use of Hydrogen as Fuel: A Trend of the 21st Century," *Energies*, vol. 15, no. 1, p. 311, Jan. 2022, doi: 10.3390/en15010311.

[45] M. Alnajideen *et al.*, "Ammonia combustion and emissions in practical applications: a review," *Carbon Neutrality*, vol. 3, no. 1, p. 13, Dec. 2024, doi: 10.1007/s43979-024-00088-6.

[46] G. B. Ariemma, G. Sorrentino, M. De Joannon, R. Ragucci, and P. Sabia, "Ammonia/Hydrogen and Cracked Ammonia Combustion," *Energy Fuels*, vol. 39, no. 40, pp. 19512–19525, Oct. 2025, doi: 10.1021/acs.energyfuels.5c02759.

[47] G. Ciccarelli, D. Jackson, and J. Verreault, "Flammability limits of NH3–H2–N2–air mixtures at elevated initial temperatures," *Combust. Flame*, vol. 144, no. 1–2, pp. 53–63, Jan. 2006, doi: 10.1016/j.combustflame.2005.06.010.

[48] S. Devkota *et al.*, "Techno-economic and environmental assessment of hydrogen production through ammonia decomposition," *Appl. Energy*, vol. 358, p. 122605, Mar. 2024, doi: 10.1016/j.apenergy.2023.122605.

[49] "Global Hydrogen Review 2025." [Online]. Available: International Energy Agency.